Synthesis and optoelectronic properties of new ethynylated pyrazine derivatives

Zhao, Liang

SYNTHESIS AND OPTOELECTRONIC PROPERTIES OF NEW ETHYNYLATED PYRAZINE DERIVATIVES

LIANG ZHAO, B.SC.

GRADUATE SOCIETY

DEPARTMENT OF CHEMISTRY

UNIVERSITY OF DURHAM

A Thesis submitted for the degree of Master of Science

at the University of Durham

October 2003

STATEMENT OF COPYRIGHT

DECLARATION

The work described in this thesis was carried out in the Department of Chemistry at the University of Durham, between October 2002 and September 2003. All the work was carried out by the author unless otherwise stated, and has not previously been submitted for a degree at this or any other university.

TABLE OF CONTENTS

ABSTRACT

Several diaryleneethynylpyrazine derivatives, in which the pyrazine unit is electron-deficient, have been synthesised using Sonogashira palladium-catalysed cross-coupling reactions. Compound **32**, an important intermediate in the synthesis of diaryleneethynylpyrazine derivatives was made by a modified literature procedure which improved the yield. Examination of optical absorption and photoluminescence spectra of compound **37** shows that the pyrazine unit does not change the behaviour significiently compared to analogue **42**, while compound **38** shows pyridine substituents have a profound effect on the photophysics of these pyrazine systems. The redox properties of representative compound **37** were studied by cyclic voltammetry, which shows that reduction of **37** to its radical anion occurs as a reversible process at high negative potentials of ca. –1.87 V. The X-ray crystal structure of **37** is also presented. Quantum mechanical calculations of the geometry and electronic structure were performed for compound **37;** the known phenylene analogue **42** was calculated at the same level for comparison. The results show that the energies of both HOMO and LUMO orbitals of **37** are decreased compared to **42.** The calculated value of the HOMO-LUMO gap of **37** (3.56 eV) is close to that estimated from the red edge of the longest wavelength absorption (382 nm = 3.25 eV).

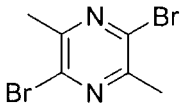

32

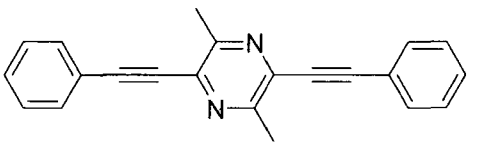

37

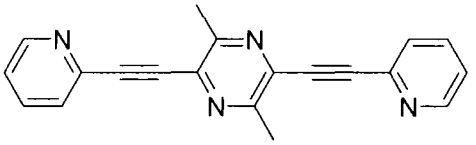

38

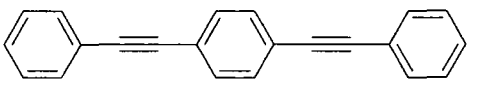

42

Acknowledgements

I would like to thank the following people who have helped and guided me through this M.Sc. at Durham: Professor Martin Bryce for offering me the opportunity to work within his group, and for his many helpful ideas, suggestions and discussion. Dr. Changshang Wang for offering his support throughout this course, Dr. Igor F. Perepichka for his help with the electronic energy calculations, Karen Samantha Findlay for help with the optical analysis, and the technical staff of the department for providing an excellent service and invaluable help.

For My Parents

Chapter One: Introduction

1.1 Conjugated polymers and oligomers

The development of conjugated polymers, e.g. polyacetylene, polypyrrole and polythiophene with interesting semiconducting properties, as a result of doping by chemical or electrochemical means, took place throughout the 1980s and 1990s and for many years research was driven by the search for metallic and even superconducting properties in these types of materials[1]. Reports of devices with potentially useful properties began to appear in the literature in the late-1980s, e.g. field effect transistors (FETs) based on electrochemically deposited poly(3-methylthiophene)[2]. It is now widely appreciated that many conjugated oligomers (rather than high molecular weight polymers) possess similar semiconducting properties, making them also suitable for device applications[3]. Extensive studies on the generation of charge carriers and electronic conduction in conjugated polymers laid the basis for what is currently one of the most exciting areas of research in conjugated organic systems, namely the development of their photoluminescent (PL) and electroluminescent (EL) properties.

1.2 Photoluminescence (PL)

Luminescence is described as light emitted by a cold excited body, in contrast with the light emitted by incandescent bodies. Because of the quantum nature of light and considering only low excitation conditions, one absorbed photon can induce at best one luminescence photon whose energy is necessarily smaller than (or equal to) that of the excited photon (Stokes' law). Luminescence can be categorised by the manner in which the excited state is formed.

Photoluminescence is the type used in spectroscopy and occurs when light is absorbed by a molecule. It can be described as a three-step process: 1. absorption of one photon of the excitation source creating in the material a primary excitation; 2. evolution of this primary excitation by energy relaxation or energy transfer toward secondary excitation at lower energy; 3. coupling of this secondary excitation to light, giving rise to the spontaneous emission of one luminescence photon. Other types of luminescence include electroluminescence (involving a reaction releasing energy as light rather than heat), and bioluminescence (for example in special organs of deep sea fish to help attract prey).

Fluorescence on the other hand, results in emission from a singlet-excited state. Here the electron is of opposite spin to the one in the ground state and so the transition is allowed resulting in a much shorter lifetime that is of the order of nanoseconds. Therefore, to the naked eye it appears that light is only emitted whilst the molecule is being excited. Photoluminescence allows the best control over the excitation conditions and for that reason is the most useful process for studying the fundamental properties of luminescent materials for fluorescent tubes and cathode-ray tubes, which took place in the 1940s. The study of photoluminescence in organic and semiconductor materials started at the end of the 1950s and developed very rapidly with the advent of lasers. The tremendous improvements in semiconductor quality linked to microelectronic applications, in terms of purity and doping control, allowed the identification of well-established luminescence mechanisms. Conversely, photoluminescence has become a very common non-destructive test of semiconductor structures.

1.3 Organic light emitting devices (OLED)

1.3.1 A brief history of electroluminescence (EL)

EL is a non-thermal generation of light resulting from the application of an electric field to a substrate[4]. In 1936 EL was first discovered for an inorganic material by Destriau et al when observing high field electroluminescence from a ZnS phosphor powder dispersed in an isolator and sandwiched between two electrodes.[5] In the 1960s and 1970s, inorganic EL gained some industrial use in EL powder lamps, and in the late 1980s in flat panel displays.

In 1963 EL for an organic material was first observed for crystals of anthracene.[6] However, the lifetimes and efficiencies of the resulting devices were significantly lower than those obtained for inorganic counterparts at the time. In 1987 a striking breakthrough occurred when the first double-layer device using organic molecular materials was reported by Tang and VanSlyke[7], and great improvement in luminous efficiency and colour tunability had been achieved. Later in 1990 the highly fluorescent conjugated polymer poly(*p*-phenylenevinlyene) (PPV) **1** was used in the formation of organic light-emitting diodes (OLEDs) by Friend et al[8]. Although PPV synthesised directly by polymerisation of its monomer is insoluble and difficult to process, Friend et al found a way to make PPV-OLEDs by the use of a soluble precursor polymer (the method is shown in Scheme 1). As a consequence of this contribution, the spin-coating method of conjugated polymer deposition was demonstrated for the first time, opening up the possibility of producing large area displays from OLED materials.

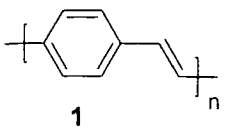

1

Compared to traditional inorganic materials, organic materials have some obvious advantages for OLEDs:

- usually OLEDs' thickness is less than 2 mm;
- the device has a wide viewing angle;
- the operating voltage of OLEDs is low;
- the colour range of OLEDs is wide;
- the power consumption is low;
- OLEDs made from polymers can be used to fabricate flexible displays.

1.3.2 The general structures and mechanism of operation of OLEDs

Under an applied voltage, oppositely charged carriers (electrons at the cathode and holes at the anode) are injected into the emissive layers from the opposing contacts, and are swept through the device by the high electric field. Some of the electrons and holes combine within the emissive materials to form triplet and singlet excited states. The singlets are distinguished from the excited states of photoluminescenece (PL), the fluorescence process resulting from photoexcitation of the ground state.

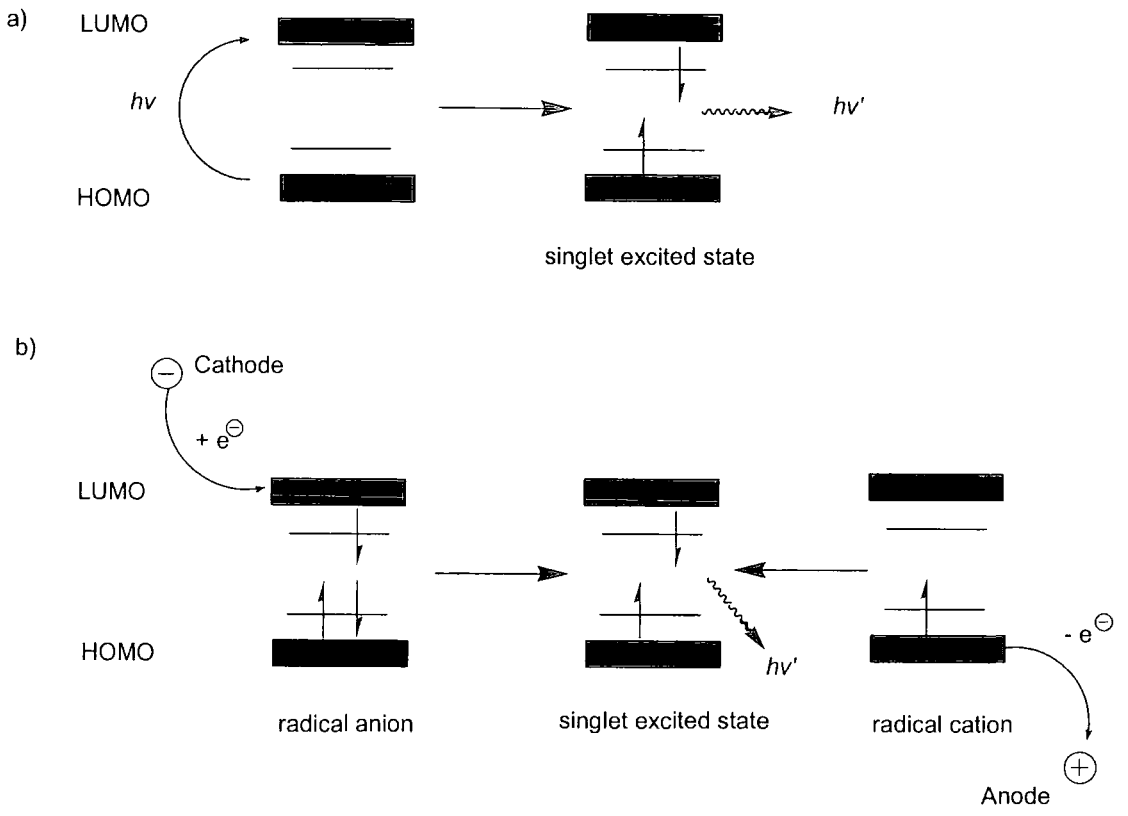

Figure 1

a) Irradiation of a fluorescent polymer excites an electron from the HOMO to the LUMO. In a typical conjugated polymer, two new energy states are generated upon relaxation within the original HOMO-LUMO energy gap and are each filled with one electron of opposite sign (singlet excited state). The excited polymer may then relax to the ground state with emission of light at a longer wavelength than that absorbed (photoluminescence).

b) In a polymer LED, electrons are injected into the LUMO (to form radical anions) and holes into the HOMO (to form radical cations) of the electroluminescent polymer. The resulting charges migrate within the polymer chains under the influence of the applied electric field. When a radical anion and a radical cation combine on a single

conjugated segment, singlet and triplet exited states are formed, of which the singlets can emit light.

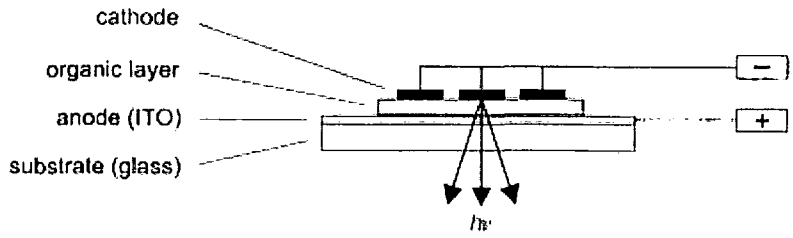

Figure 2 Single layer devices ITO: indium tin oxide.

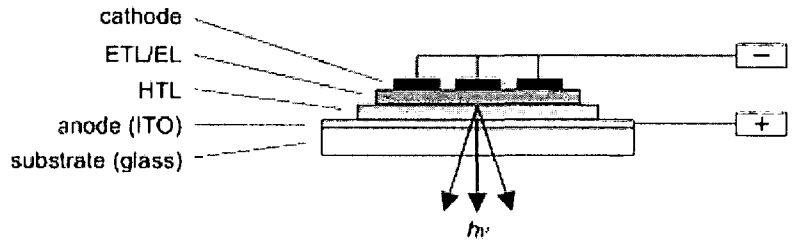

Figure 3 Multi-layer devices ETL: electron transport layer; EL: emitting layer; HTL: hole transport layer.

One of the potential important usages of OLEDs is to make coloured flat panel displays; there are several ways[9] to realize this goal.

a) Blue, green, and red OLEDs

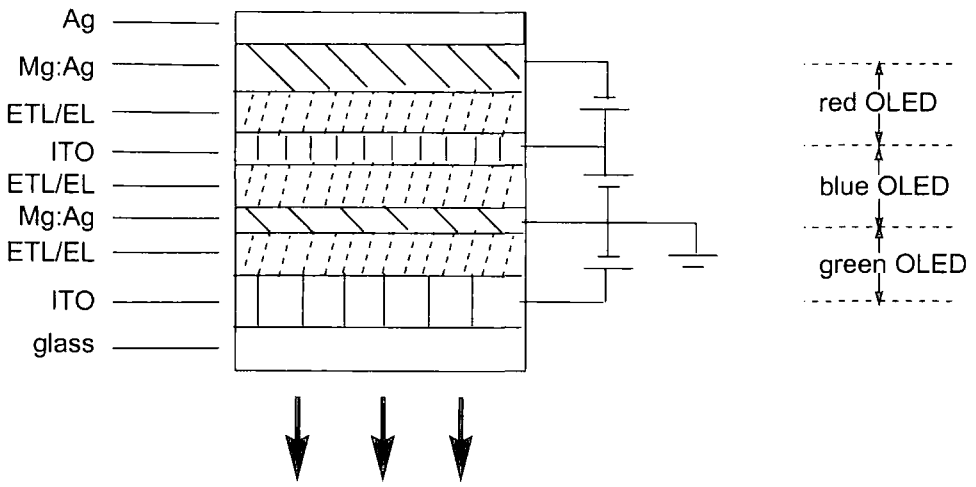

Figure 4

b) OLEDs tunable from blue to red emission based on the voltage, current, local temperature, or another device parameter

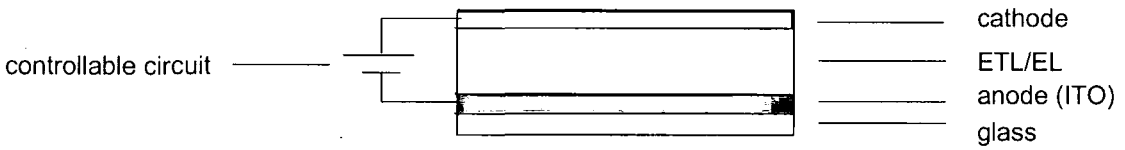

Figure 5

c) OLEDs with a spectrally broad white emission, covered with red, green, or blue absorption filters (figure 6)

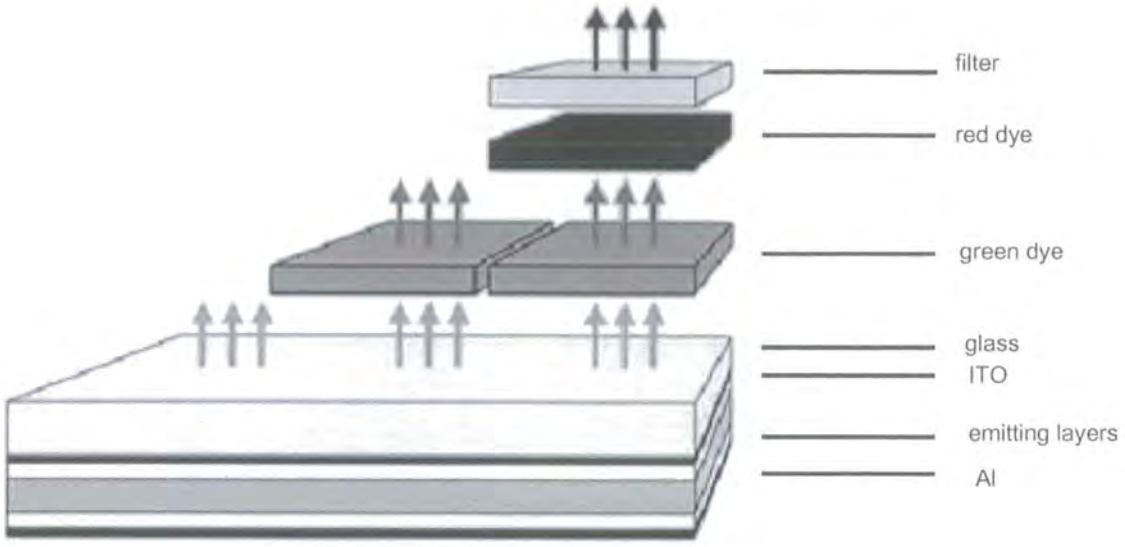

Figure 6

1.3.3 Low molecular weight materials

As stated above, the basic requirements for organic electroluminescent materials are electron and hole transport, recombination of electrons and holes and fluorescence efficiency. With respect to their molecular structure they can be classified into three groups: namely, low material weight, polymeric and oligomeric materials.

Two-layer OLEDs were first assembled by Tang and VanSlyke at Kodak Laboratories in 1987.[7] The device contains two layers: **2** and **3** (Alq_3) of different charge carrier transport properties. Compound **3** is used for electron transport and at the same time as an emitting layer, but it is unable to carry holes. In contract, bis(triarylamine) derivative **2** was inserted to provide efficient hole transfer. So charge recombination was largely confined within a region very close to the interface between both organic materials, and in this way lead to high

external quantum efficiencies (1%), luminous efficiencies (1.5 lm W^{-1}) and brightnesses (>1000 cd m^{-2}).

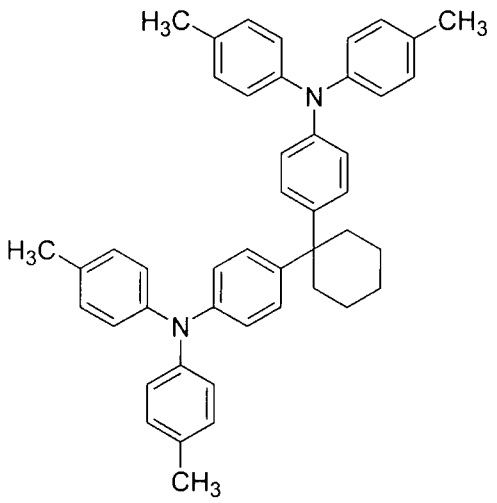

2

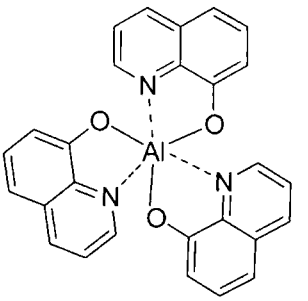

3

As most small molecular materials can only have one or two specific functions required for OLEDs (such as fluorescence, electron and hole transport) multilayer devices are fabricated to achieve improved results. According to their function in the EL devices, low molecular weight materials can be classified into five groups:

- electron transport emitters;
- dopant emitters;
- electron transport and hole blocking materials;
- hole transport materials;
- electron and hole transport emitters.

1.3.3.1 Electron transport emitters

Metal chelates, for example compound **3** (Alq_3), are the most common electron transport emitters used in the fabrication of organic devices. The photoluminescence efficiency of Alq_3 thin films is around 32%.[10] In order to change the emission wavelength and the energetic position of the frontier orbital, many derivatives of Alq_3 have been synthesized and their physical characteristics studied.[11]

Besides Alq_3 and its derivatives, other metal chelates[12], lanthanide[13] and boron[14] complexes have also been studied as electron transport emitters in OLEDs. Zinc complex **4** revealed a yellow luminance of 16 200 cd m^{-2} in a standard device configuration (ITO/TPD **13**/**4**/Mg:In).[15] One of the most remarkable electron transport emitters besides Alq_3 is beryllium complex **5**, which achieved a brightness of 19 000 cd m^{-2} and a luminous efficiency of 3.5 lm W^{-1} in a two-layer device configuration (ITO/TPD/**5**/Mg:In).[16] Lanthanide complexes of the general structure **6** have been used as luminescent dopants and electron transport emitters in EL devices with external quantum efficiencies up to 1%.[17] Spectral narrowing and luminescence enhancement were reported for multilayer structures based on europium and terbium complexes.[18]

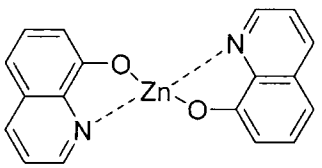

4

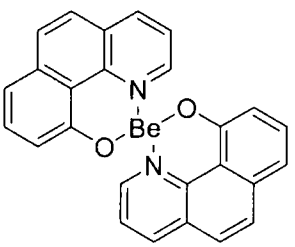

5

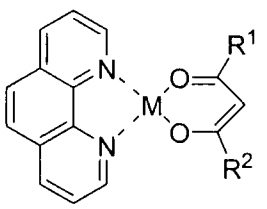

M = Tb, Eu, Dy, Gd
R^1 = CH_3, phenyl, 2-thienyl
R^2 = CH_3,CF_3, phenyl

6

1.3.3.2 Dopant emitters

Solid-state organic fluorescent dyes tend to suffer from various degrees of quenching which typically causes broadening and bathochromic shifts of the emission bands. These problems can be overcome by doping or dispersing fluorescent dyes as guests within a host matrix, which typically serves as a hole and/or an electron transport material. In this way, self-quenching can be minimized. To achieve high electroluminescene efficiency, there are three criteria to follow.

- the materials should be evaporable and exhibit high fluorescence quantum yields;
- energy levels of the host and the guest should be complementary;
- narrow emission bands of the dopants are favourable to maintain chromatic purity.

Tang et al dramatically raised the external quantum efficiency of their ITO/**2**/Alq_3/Mg:Ag device to a value of 2.5% by doping the Alq_3 layer with small amounts of compounds **7** or **8**.[19] However, if the concentration of dopant is too high, the devices' performance will be affected unfavourably.

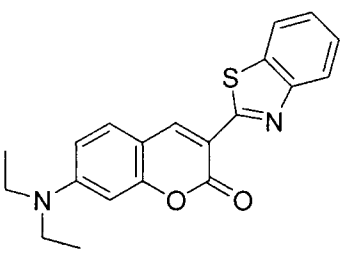

7

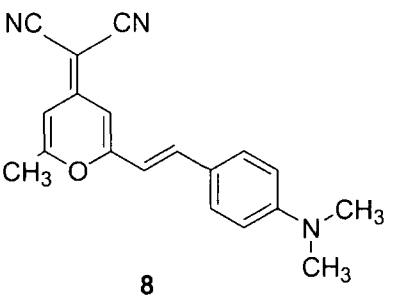

8

The most frequently used dopant is rubrene **9**. Compared to analogous undoped devices, improved stability and a doubling of the luminous efficiency to 2.35 lm W^{-1} have been

achieved by doping 5 wt% rubrene into the TPD layer of a simple two-layer device (TPD **13**: **9**/Alq_3/Mg:Ag).[20]

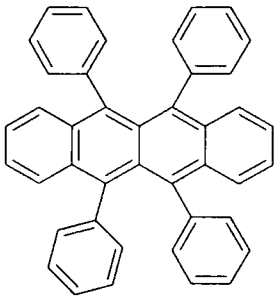

9

1.3.3.3 Electron transport and hole blocking materials

1,3,4-Oxadiazole derivatives possess the important properties for device fabrication of forming uniform thin films by vacuum sublimation and exhibiting large ionisation potentials for efficient hole blocking.[21] The most important low molecular weight compound of this family is 2-biphenyl-4-yl-5-(4-*tert*-butylphenyl)-1,3,4-oxadiazole **10** (PBD), first utilized by Tsutsui et al. [21b, 22]

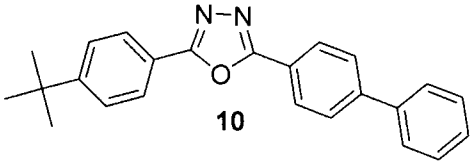

10

1,3,4-Triazoles are another interesting class of electron-deficient thermostable materials similar to oxadiazoles. Triazoles were first used by Kido et al as electron transporting and

hole blocking materials.[23] The most representative derivative is 3-(1,1′-biphenyl-4-yl)-5-(4-*tert*-butylphenyl)-4-phenyl-4*H*-1,2,4-triazole **11**, which is not only a good electron transporter but also a better hole blocker than PBD **10**.[19]

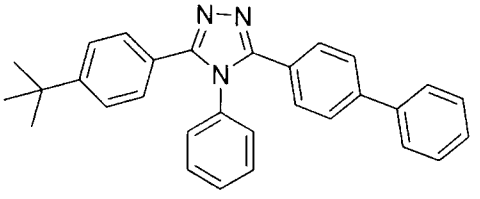

11

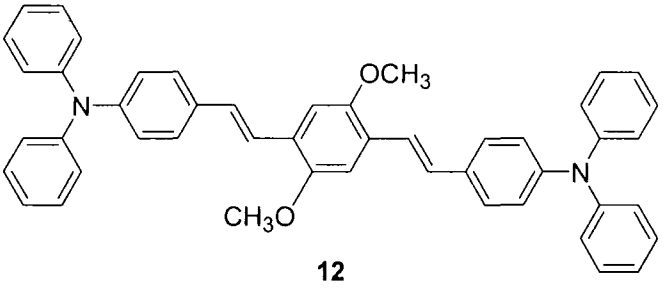

12

Taking advantage of the hole blocking qualities of triazole **11**, Hörhold et al. fabricated a highly efficient three-layer device (ITO/TPD/**11**:**12**/**11**/Ca:Al) with a luminous efficiency of 3 lm W^{-1}, a maximum brightness of about 5500 cd m^{-2} and a luminance of 500 cd m^{-2} at moderate voltages (7 V).[24]

1.3.3.4 Hole transport materials

A numerous array of materials have been developed as hole transport materials in OLEDs. *N*,*N*′-Diphenyl-*N*,*N*′-bis(3-methylphenyl)-1,1′-biphenyl-4,4′-diamine (TPD) **13** and *N*,*N*′-

bis(1-naphthyl)-*N*,*N*′-diphenyl-1,1′-biphenyl-4,4′-diamine (NPD) **14** have been extensively studied in this context.[25]

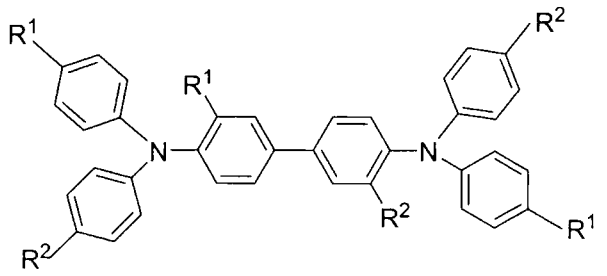

13 R^1 =CH_3 R^2=H

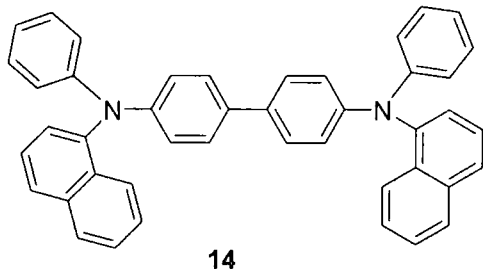

14

1.3.3.5 Electron and hole transport emitters

With the aim of achieving both efficient charge transport and fluorescence in a single molecule, several structures incorporating both electron transporting oxadiazole units and hole transporting diphenylamine groups have been synthesized. The most efficient device was based on compound **15** with Alq_3 as the electron injecting layer.[26] An external quantum efficiency of 4%, a luminous efficiency of 3.75 lm W^{-1}, and a maximum luminance exceeding 19 000 cd m^{-2} was achieved in the most successful device based on this compound. However, the durability of the device under operating conditions was disappointing (the initial brightness decayed to half its intensity in less than 1 h).

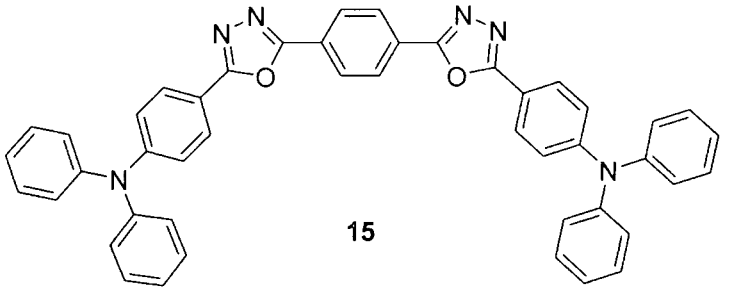

15

1.3.4 Conjugated polymers in OLEDs

An attraction of low molecular weight materials or small oligomers is that they can frequently be purified by column chromatography or recrystallisation and their molecular structures can be unambiguously characterised by standard analytical techniques (NMR spectroscopy, elemental analysis, single crystal X-ray diffraction, etc.). However, their main disadvantage is the expensive and technologically inconvenient process of vapour deposition required to make thin films. In comparison, conjugated polymers are much easier to process and at the same time can exhibit good fluorescent properties.

PPV was the first extensively studied polymer in this context. PPV is a bright yellow, fluorescent polymer, with an EL emission maximum at λ 551nm (2.25 eV) and 520 nm (2.4 eV) in the yellow-green region of the visible spectrum.[8] However, PPV synthesized directly from a monomer is insoluble, intractable, and infusible, making the material very difficult to process. The problem was solved by preparing PPV via a processable precursor polymer (scheme 1).

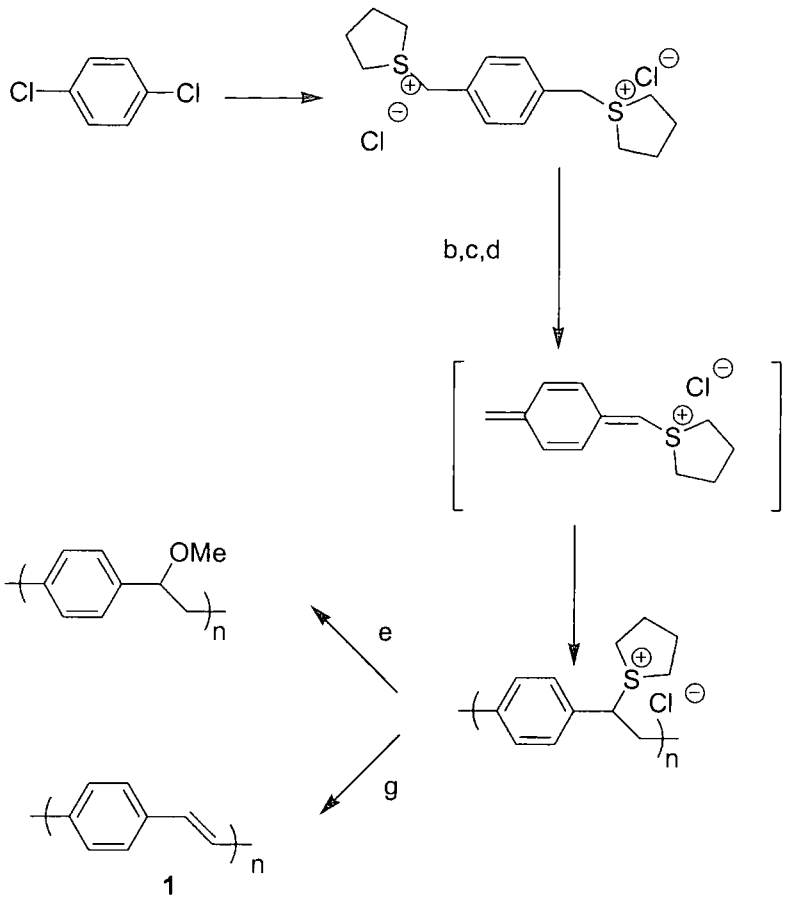

synthesis of PPV a) terahydrothiophene, MeOH, 65°C; b) Na OH, MeOH/H_2O or Bu_4NOH, MeOH,0°C c) neutralization (HCl); d) dialysis (water); e) MeOH, 50°C; f) 220°C, HCl (g) Ar, 22h; g) 180-300°C, vacuum, 12h.

Scheme 1

The introduction of substituents into the PPV skeleton has also enabled the generation of PPVs that are soluble in a range of standard organic solvents. In 1991, Braun and Heeger reported a red–orange emitting OLED based on the unsymmetrically substituted soluble PPV derivative poly[2-methoxy-5-(2-ethylhexyloxy)-*p*-phenylenevinylene] (**16**), [27] and this material has remained as the bench-mark polymer for most EL device studies. A variety of PPV derivatives containing long alkyl and alkoxy chains, cholestanyloxy and oligoethenyloxy substituents have been synthesized by polycondensation, Wittig-, or Heck-type reactions.

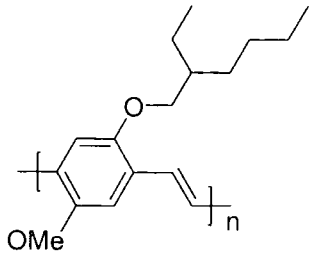

16

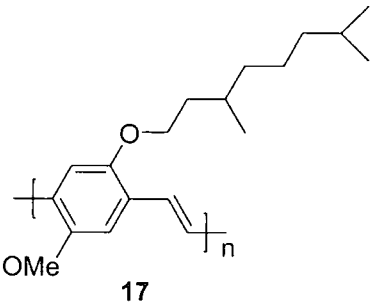

17

Up to now, the highest external quantum efficiency that has been obtained for a single-layer OLED is 2.1%.[28] This OLED, developed at Philips laboratories in 1996, was based on dialkoxy-substituted PPV derivative **17** and possessed a brightness of 100 cd m^{-2} with a luminous efficiency of 3 lm W^{-1} at an operating voltage of 2.8 V.

Conjugated polymers tend to have low electron affinities making electron injection more difficult than hole injection. One way to overcome the problem is by the attachment of electron withdrawing cyano groups to the vinylene bonds of PPV. CN-PPV **18** was studied by Friend and Holmes et al[8]. Internal efficiencies of 0.2% were reported for a single-layer configuration Al/CN-PPV/metal (Al or Ca). Several other electron withdrawing substituents have been tried, although none surpasses CN-PPV.

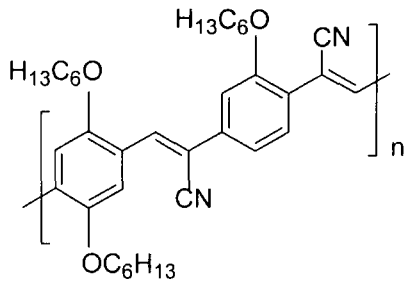

18

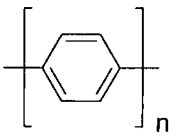

19

The fabrication of blue inorganic LEDs is difficult and expensive, therefore, blue emission is of considerable importance in OLED research. Blue OLEDs were first reported by Leising et al in 1992 using poly(*p*-phenylene) (PPP) **19** as the active layer in the device[29] to obtain external quantum efficiencies for simple single-layer devices of 0.05%.

Similar to PPV, PPP is also hard to process due to its insolubility and infusibility. In order to improve processability, PPP derivatives bearing solubilizing side chains, such as alkyl, aryl, alkoxy, or perfluoroalkyl, have been synthesized.[30] However, a drawback associated with this substitution is that the presence of the chains leads to increased distortion of adjacent rings, which causes a blue-shift of the emission which is often accompanied by a reduction of fluorescence quantum yield. In an effort to overcome these problems, Scherf and Müllen et al developed ladder-type PPP derivatives **20-22** which comprise a rigid planarized polymer backbone.[31] The best performance reported to date for PPP-based diodes with an external efficiency beyond 4% was achieved with a blend of ladder-type polymer **21b** and small amounts of poly(3-decylthiophene) **23** in a single-layer configuration (ITO/**21b**:**23**/Al).[32]

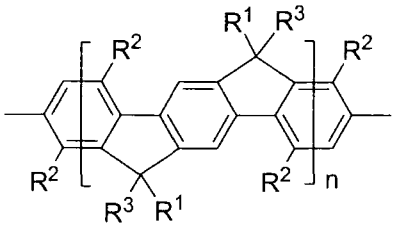

20 R^1 = H, R^2 = C_6H_{13}, R^3 = *p*-*t*BuC_6H_4 (a), *p*-$C_{10}H_{21}C_6H_4$ (b)
21 R^1 = CH_3, R^2 = C_6H_{13}, R^3 = *p*-*t*BuC_6H_4 (a), *p*-$C_{10}H_{21}C_6H_4$ (b)

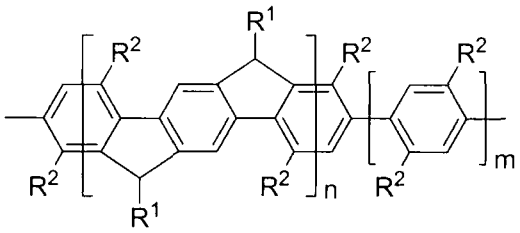

22

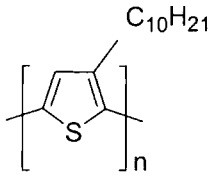

23

1.3.5 Oligomers

In general, oligomers have similar physical properties and processability suitable for the fabrication of devices. However, they are different from conjugated polymers, which have randomly dispersed defects leading to a statistical distribution of lumophore lengths. Oligomers provide strict control of the effective conjugated length as a result of their controlled synthesis, thereby providing more precise control of the absorption and emission properties. Therefore, oligomers are routinely synthesized as model compounds to study structure/property relationships in the corresponding polymers. However, on account of their controllable and rigorously defined structure, conjugated oligomers have also been used as novel materials in their own right and as alternatives to polymers in electrooptical applications.

1.4 Trends and future of OLEDs

From the late 1990s, many properties of OLEDs have begun to meet the requirements for application in displays. The luminance has reached 100 cd m^{-2} with a luminous efficiency of 10 lm W^{-1}. However, the life-time of OLEDs still needs improvement. For most applications, operating lifetimes should be above 10,000 hours and minimum storage times of five years are required. After rigorous study of device architectures and optimization of the emitting material, a deeper understanding of degradation and device failure mechanisms can be gained. Solid state morphology is decisively important to both lifetime and efficiency. Layer-wise topographic analyses of OLEDs have been carried out using scanning electron microscopy (SEM), transmission electron microscopy (TEM), atomic force microscopy (AFM), and scanning tunneling microscopy (STM) as analytical methods.[33] Besides lifetime, "black spots" are another problem for commercial usage of OLEDs in displays. These are caused by local electrical short-circuits[34]. Their occurrence was found to be accompanied by morphological changes that lead to delamination of the semiconductor film from the metal surface. Long-term loss of efficiency of OLEDs associated with the decrease of quantum efficiency and luminance along with an increase in voltage, while the device is stressed under constant current, has been attributed to impurities in the emissive zone, introduced either during device fabrication or produced by electrochemical reactions[35].

As a whole, OLEDs have been greatly improved during the last few years with respect to reliability, efficiency and tunability, and are now commercially competitive to their inorganic counterparts in some cases. Currently, devices based on conjugated polymers and low molecular weight materials compete for prevalence in the field of organic

electroluminescence, and the optimisation of diodes based on both types of materials is proceeding rapidly. The polymer approach seems to be less sensitive to higher temperatures and affords the promise of much lower fabrication costs. Whilst the production of sublimed molecular film devices typically requires vapor deposition, conjugated polymers offer the possibility of manufacturing large area displays by simple roll-to-roll coating techniques. However, the two concepts are not mutually exclusive, since combinations of both approaches have already been demonstrated. For the near future, it appears that both technologies with their specific advantages and drawbacks will coexist and develop side-by-side with each other. Although efficiency and durability of devices still need to be further improved with respect to high-end applications, the prospects are that these obstacles are not insurmountable and will soon be overcome if the current rate of progress continues.

1.5 The choice of target product

Conjugated polymers based on electron-deficient heterocyclic units, in particular systems containing electron-withdrawing imine nitrogen atoms (C=N), have attracted considerable interest as electron-transporting layers in the fabrication of multilayer devices.
Polyheterocycles with high electron affinities enable the construction of highly efficient OLEDs, even with air-stable electrodes. As examples, the efficiency of multilayer devices is significantly improved by using poly[2,2'-(*p*-phenylene)-6,6'-bis(3-phenylquinoxaline)] (PPQ) **24** as electron transit layer. [36]

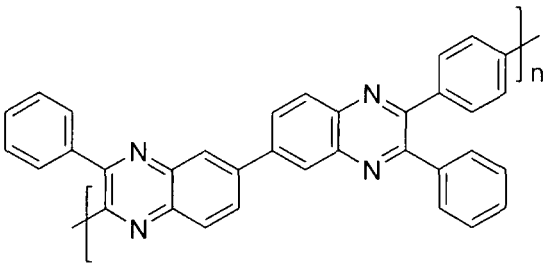

24

Pyridine derivatives have been applied in blue-emitting devices, as the electron-deficient moiety[37]. Compared to benzene, pyridine is an electron-deficient aromatic heterocycle, with a localized lone pair of electrons in an sp^2 orbital on the nitrogen atom; consequently, the derived polymers have increased electron affinity, improved electron-transporting properties, and the symmetry of poly(phenylene) systems is broken. Polymer **25** was synthesized as electron-transporting layers in LEDs[38].

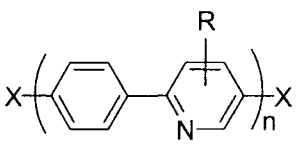

25

R = n-C_6H_{13} X = Br (a), Ph (b)

Polymers **26** (a-c) were made to combine the merits of PPP and polypyridine (PPy)[39]

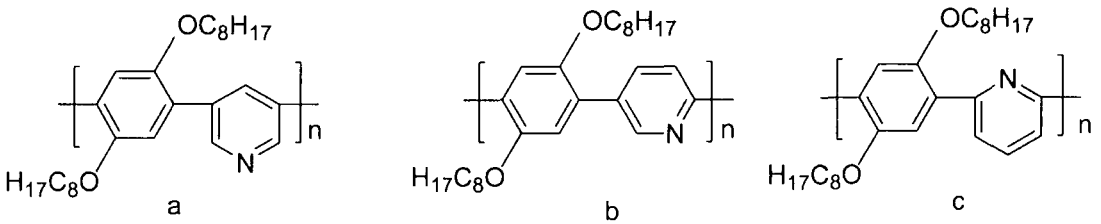

a b c

26

Conjugated oligomers with an alternating phenylene-pyrimidine structure have been synthesized[40]. Blue light-emitting electroluminescent devices with an external quantum efficiency up to 1.8% have been fabricated by using compound **27** as the emitting layer.

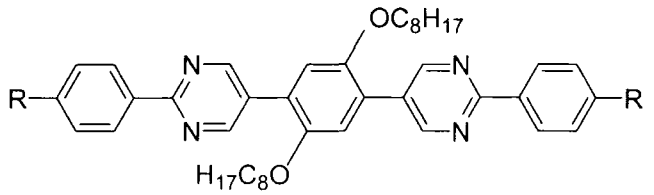

27

R = H (a), OC_4H_9 (b), t-Bu (c)

Compound **28,** with a similar pyrazine system was also reported[41].

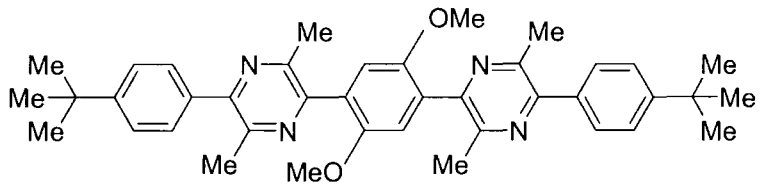

28

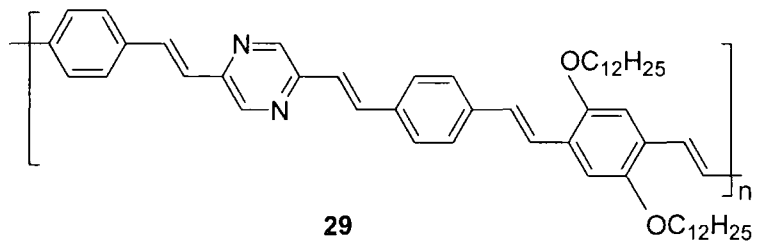

29

The electron injection is significantly improved in OLEDs made with polymer **29**, which contains a pyrazine unit in the backbone, compared to alkoxy-substituted PPV derivatives.[42]

My work which is described in the following chapters has focussed on the synthesis and properties of new pyrazine derivatives, which is a heterocycle hitherto largely ignored as a component of luminescent materials.

Chapter Two: Results and Discussion

2.1 Introduction

As discussed in Chapter one, we sought to explore new electron-transporting materials and we recognised the following potential advantages of pyrazine derivatives in this context.

- The heterocycle is electron-deficient;
- It can be symmetrically functionalised;
- The optoelectronic properties, including luminescence, of its derivatives are largely unexplored.

Herein we describe our work on 2,5-dibromo-3,6-dimethylpyrazine **32** as the starting material for the synthesis of a series of new pyrazine derivatives and an exploration of their structural and optoelectronic properties. We targeted a series of diaryleneethynylpyrazines for our studies, because there is much current interest in oligoaryleethynylenes as highly conjugated molecules with potential uses as molecular wires and in light emitting devices[43]. The alkyne bond can be considered as having cylindrical geometry, which helps to maintain conjugation along the molecular axis from one aromatic ring to the next. The extent of this conjugation will be influenced by twisting of the aromatic rings out of the overall plane, with more twist leading to less conjugation and hence lower intramolecular conductivity[44].

2.2 Synthesis of 2,5-dibromo-3,6-dimethylpyrazine 32

Although 2,5-dibromopyrazine is known,[45] previous work in our laboratory[46] had failed to reproduce the literature synthesis (namely, a Sandmeyer reaction on 2-amino-5-

bromopyrazine) in sufficient yield to provide enough material for further reactions. We, therefore, chose to use 2,5-dibromo-3,6-dimethylpyrazine **32** as our starting reagent. An outline synthesis has been reported for this compound, although details in the literature are lacking.[47]

The starting material is commercial alanine anhydride **30**. Reaction of **30** with a mixture of phosphoryl chloride and phosphorus pentachloride at 105 °C is reported to give 2,5-dichloro-3,6-dimethylpyrazine **31** in 12% yield[48]. We repeated this reaction and obtained **31** in a yield of 30%. Conversion of compound **31** into the dibromo analogue **32** using phosphorus tribromide gave the desired product in 31% yield[49]. In a typical reaction we obtained 1.0 g of analytically pure compound **32**, and this appears to be the good scale for this reaction.

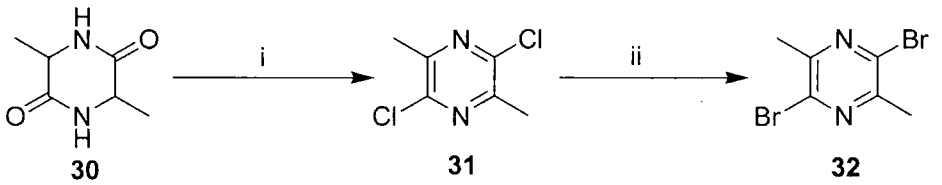

30 **31** **32**

Scheme 2

i $POCl_3$, PCl_5, 105 °C, 24 h

ii PBr_3, 170 °C, 24 h

2.3 Catalysed reactions to diaryleneethynylpyrazine derivatives

Having developed a reliable route to compound **32** we were able to explore displacement of the bromine atoms in Sonogashira palladium-catalysed reactions to obtain diaryleneethynylpyrazine derivatives, which are hitherto an unexplored family of compounds.

The Sonogashira coupling reaction[50] proceeds via the catalytic cycle shown in Scheme 3. The reaction is usually performed under an inert atmosphere of nitrogen or argon as the presence of any oxygen can lead to homocoupling of the acetylene component to give diynes[51]. Because both bromide sites are reactive sites in compound **32** , we can get two different products respectively, by changing the ratio of reactants.

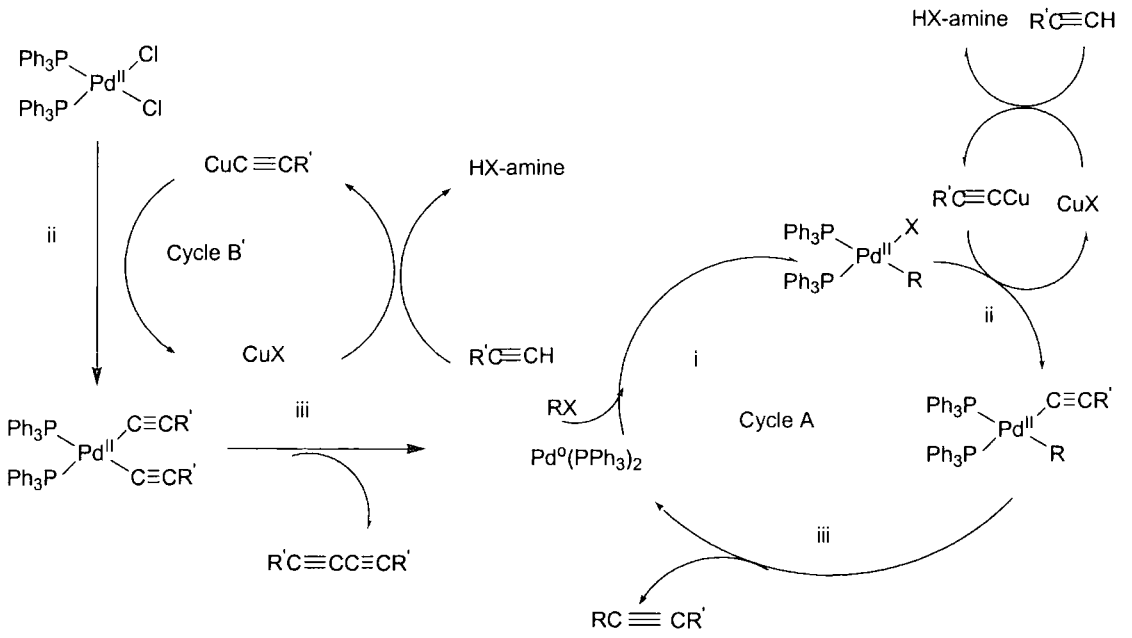

Scheme 3

Pd-catalyzed cross-coupling reaction of terminal acetylenes with sp^2 halides: i, oxidative addition; ii, transmetallation; iii, reductive elimination.

Initial reactions concerned cross-coupling of **32** with 2-methyl-3-butyn-2-ol, and products **33** and **34** were obtained arising from displacement of one or both of the bromine atoms, respectively, with yields of 35% and 36%. Treatment of **33** and **34** with base gave the unsubstituted alkyne products **35** and **36** (Scheme 4), with yields of 23% and 25%.

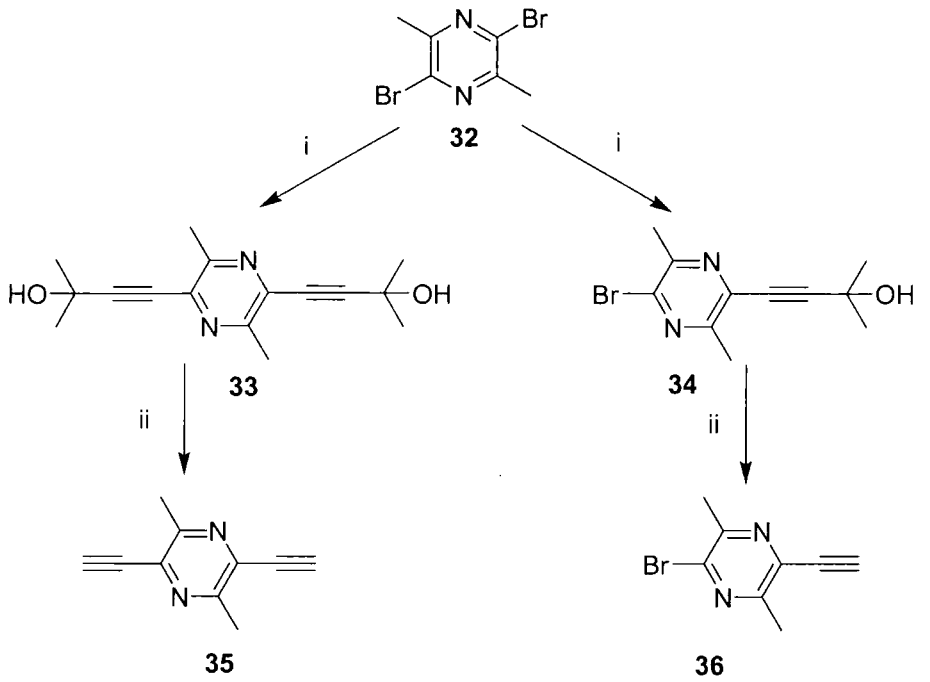

Scheme 4 : i 2-Methyl-but-3-yn-2-ol, $Pd(PPh_3)_2Cl_2$ as catalyst 65 °C, 1 h

ii NaOH in THF, 130 °C, 2 h

Similarly, 2,5-dibromo-3,6-dimethylpyrazine **32** reacted with two equivalents of a series of arylalkyne derivatives to give the corresponding diaryleneethynylpyrazine products shown in Scheme 5 .

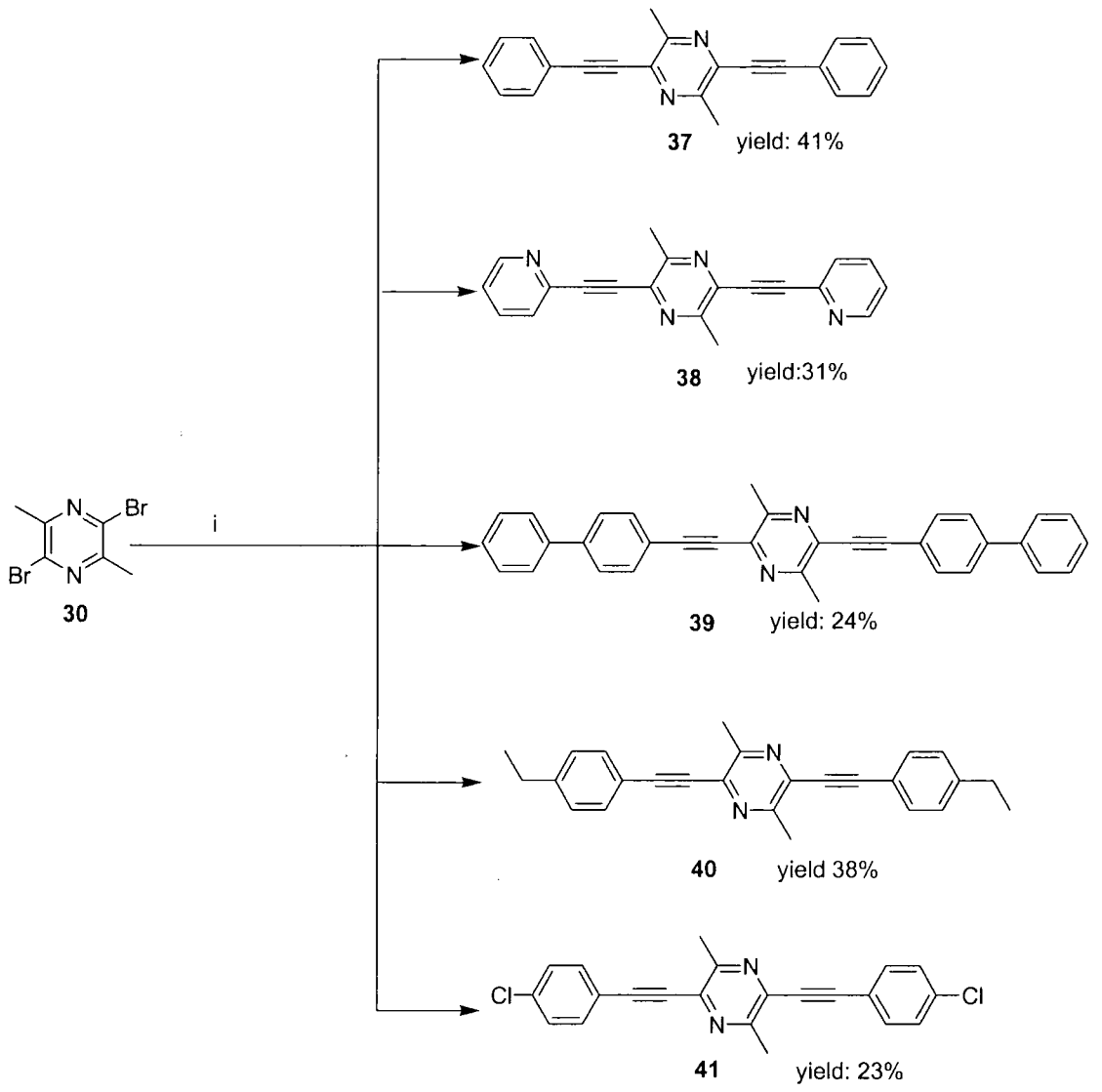

Scheme 5

i 2-Methyl-but-3-yn-2-ol, $Pd(PPh_3)_2Cl_2$ as catalyst, 65 °C, 1 h

2.4 Properties of diaryleneethynylpyrazine derivatives

2.4.1 NMR

Of this series of compounds, 2,5-dimethyl-3,6-bis(phenylethynyl)pyrazine **37** was the most extensively studied. Its ^{13}C NMR spectrum is shown in Figure 6.

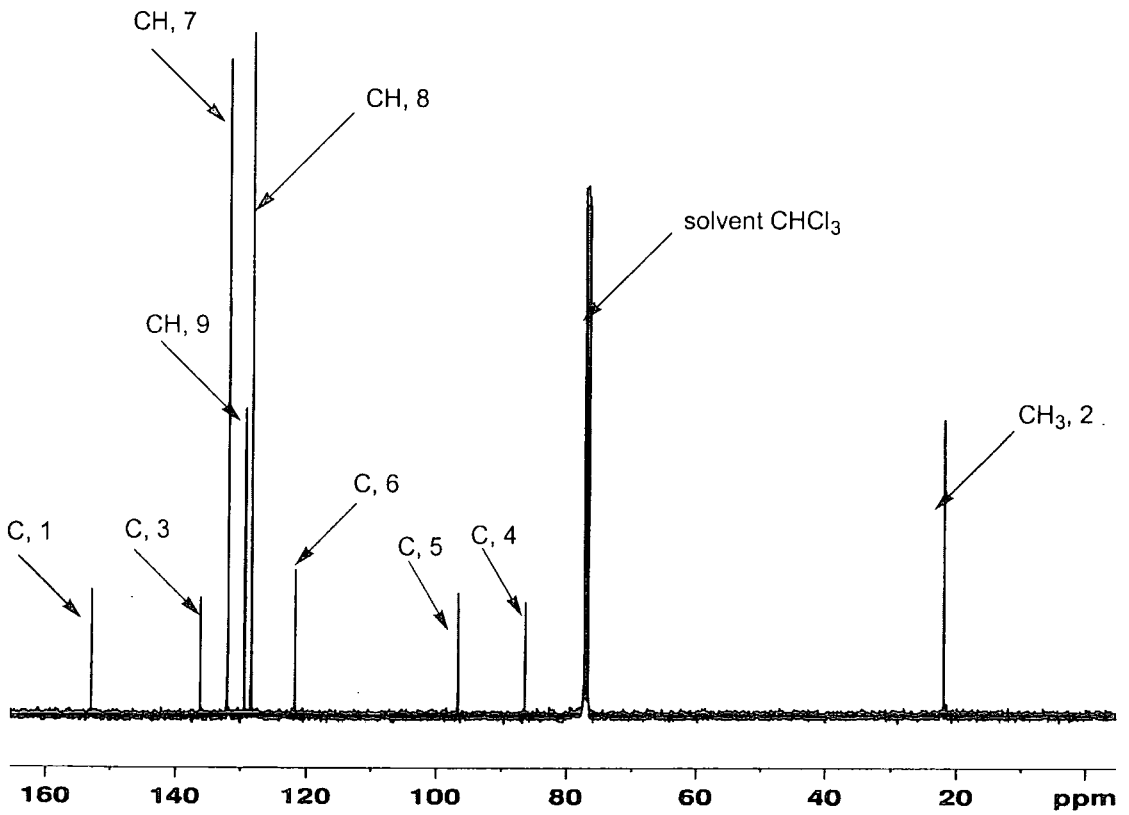

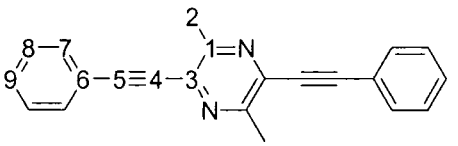

Figure 7 ^{13}C NMR spectrum of coumpound **37** in $CDCl_3$

2.4.2 Crystal structure

Crystals of compound **37** were grown from hexane solution and the X-ray crystal structure was solved by Dr Andrei Batsanov. The molecule of **37** (Fig. 8) is located at a crystallographic inversion centre. Thus the two phenyl rings are parallel, but the pyrazine ring is inclined to their planes by 14.2°. Molecules in the crystal form a layer of a brickwork

pattern (Fig. 8), parallel to the (0 0 1) plane. The long axes of all molecules, belonging to the same layer, are strictly parallel, while those in the adjacent layers are inclined to the latter by ca. 45°. In fact, packing within the layer is not particularly close, due to the non-planar conformation of the molecule. The separation between the mean planes of contacting molecules (3.49 Å) and the shortest intramolecular C...C distances (3.46–3.48 Å) correspond to normal van der Waals contacts. A phenyl ring of one molecule overlaps with the pyrazine ring of another, but the overlap is only partial (Fig. 9).

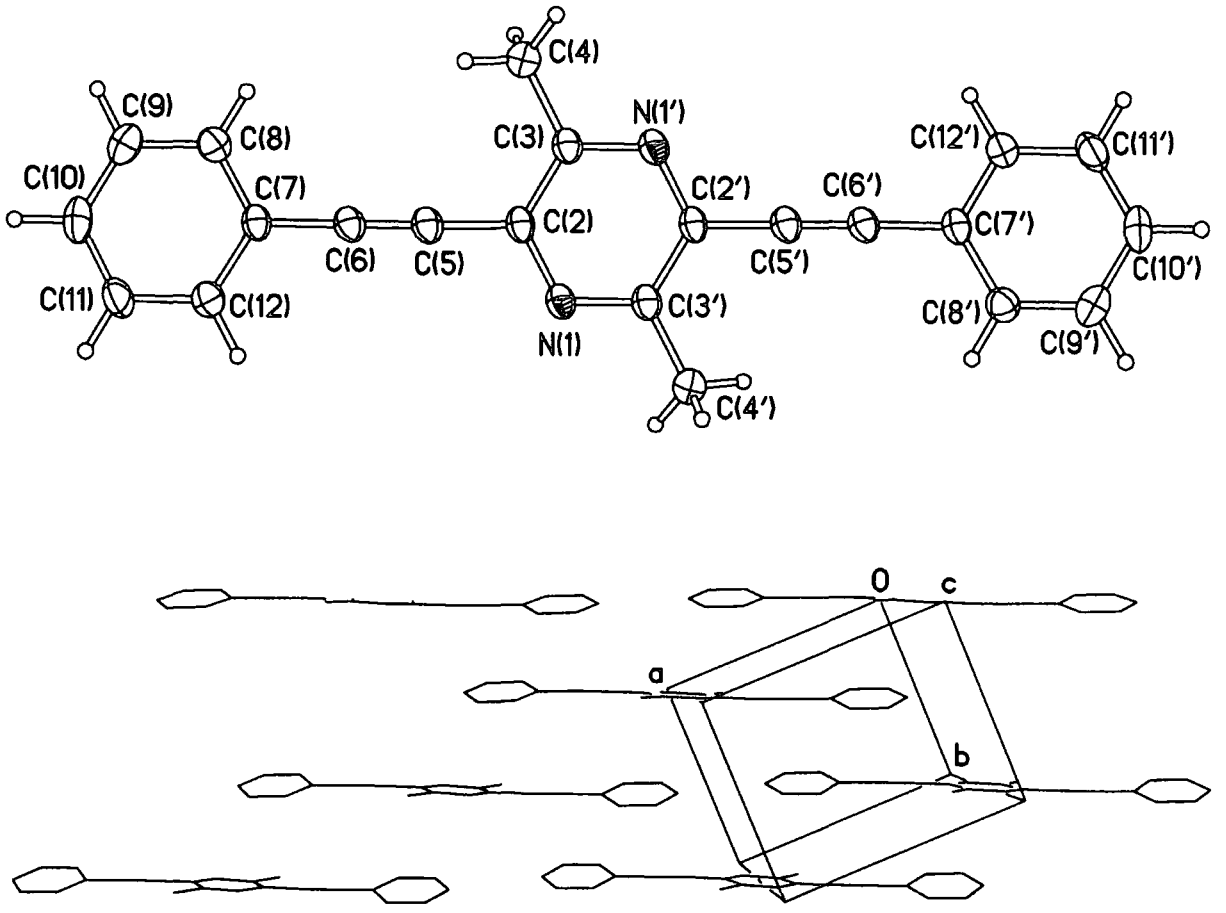

Figure 8: Molecular structure of **37**. Thermal ellipsoids are drawn at 50% probability level. Atoms, generated by the inversion center, are primed. Bottom: layer of molecules in the crystal structure; projection on the (0 0 1) plane.

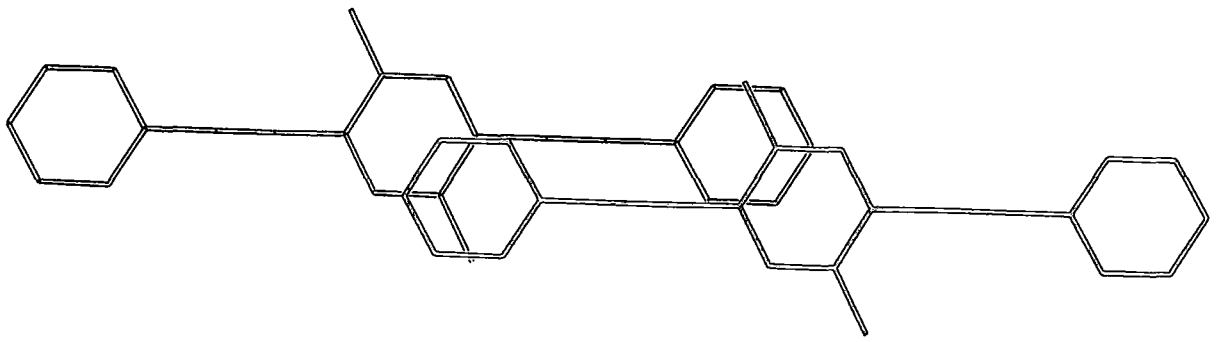

Figure 9 Overlap of molecules of **37** within a layer.

2.4.3 Quantum chemical calculations

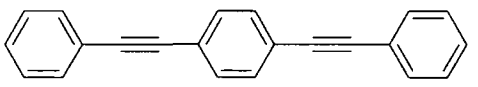

42

We also performed quantum mechanical calculations of the geometry and electronic structure for compound **37.** The geometry and the electronic structure of **37** was calculated by DFT methods at the B3LYP/6-311G(2d,p) level of theory. For reference, the known phenylene analogue **42**[43d] was calculated at the same level and both these results were compared with X-ray diffraction single crystal structures for both compounds. Both calculated structures, **37** and **42**, are essentially flat and all three aromatic rings lie in the plane. There is generally a good agreement between the calculated and the X-ray experimental bond distances: mean discrepancies are 0.006 and 0.007 Å, respectively (Fig. 10), which are in the range of the accuracy of X-ray experiments. The calculated triple bonds are somewhat longer (by 0.003–0.008 Å) and the single bonds (between the aromatic rings and sp-hybrid carbon atoms) are somewhat shorter (by 0.008–0.012 Å) than found in experiments, but again this is a quite reasonable difference between theory and experiment, taking into account that the first is for an isolated molecule in a gas phase, and second one is for a condensed matter structure.

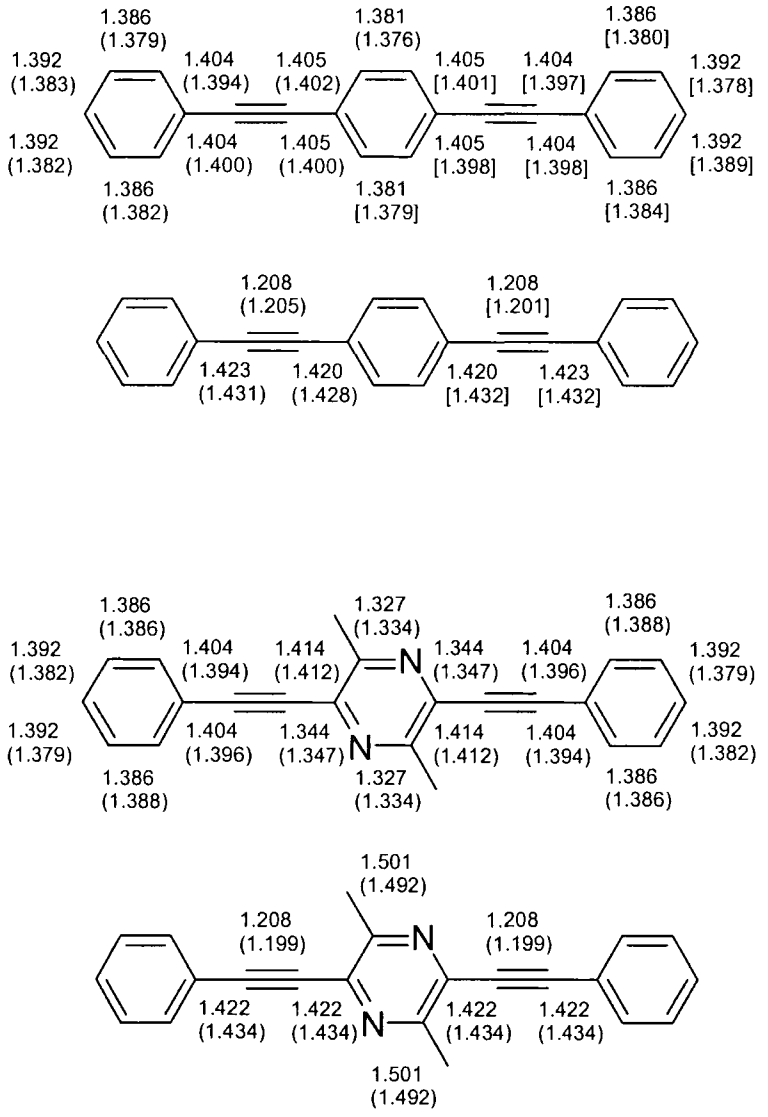

Figure 10 **B3LYP**/6-311G(2d,p) calculated bond distances in phenylene **42** and dimethylpyrazine **37** derivatives. Bond distances from X-ray analysis are given in parentheses for comparison (distances for two independent molecules from X-ray crystal structure of phenylene derivative **42** are given in parentheses and square brackets, respectively[52]). The top figures shows bond distances in the rings and bottom figures show acyclic bond distances.

Orbital energy level analysis indicates that for pyrazine derivative **37** (as compared to **42**) the energies of both HOMO and LUMO orbitals are decreased (by 0.17 and 0.33 eV, respectively) with, as expected, more pronounced changes in the LUMO energy due to the electronegative nitrogen atoms. As a result the HOMO-LUMO gap (E_g) is contracted by 0.17 eV, from 3.72 eV for **42** to 3.56 eV for **37**.

For compound **42** the HOMO is located on the C–C triple bonds as well on the central 1,4-phenylene ring, with only minor population on the end phenyl moieties. The main population at the central ring is on C–1 and C–4, which form bonding orbitals with adjacent carbons. In **37**, the HOMO is also located on the triple C–C bonds and on the central ring. The electronegative nitrogen atoms in the pyrazine ring result in somewhat different localization of the HOMO on it, exclusively on ring's carbon atoms resulting in quinoidal-type population. The LUMO in **42** populates the exocyclic C–C single bond and C–2,3, C–5,6 bonds of the phenylene ring resulting in quinoidal central moiety. Similar localization of the LUMO on exocyclic C–C single bonds is observed for **37**, whereas on the central pyrazine ring the LUMO is localized on nitrogen atoms (Fig. 12)

Population of unoccupied molecular orbitals LUMO+1 to LUMO+4 is similar for both molecules (Figure 13), **42** and **37**: LUMO+1 is shifted to the end phenyl rings which become essentially quinoidal; LUMO+2 is localized on the central ring forming antibonding orbitals between C2–C3, C5–C6 and N1–C6, C3–N4 for **42** and **37**, respectively. Structures LUMO+3 and LUMO+4 for both compounds are near the same, with population on the terminal phenyl rings. For occupied HOMO–1 to HOMO–4 orbitals, the structures of HOMO–1, and HOMO–3 orbitals for both compounds are quite similar, whereas a big

difference is observed for HOMO–2, which is quinoidally localized on the end phenyls in **42** and on the central pyrazine ring in **37**, involving participation of methyl groups and the lone pair of nitrogen atoms.

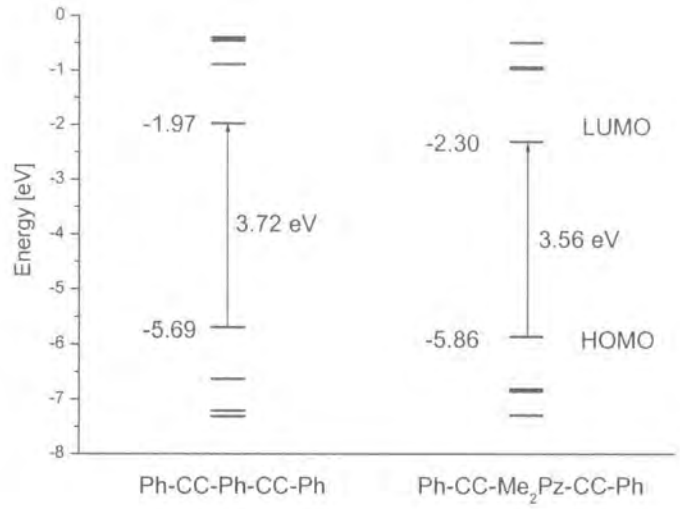

Figure 11 B3LYP/6-311G(2d,p) orbital energy levels diagrams for phenylene **42** and dimethylpyrazine **37** derivatives.

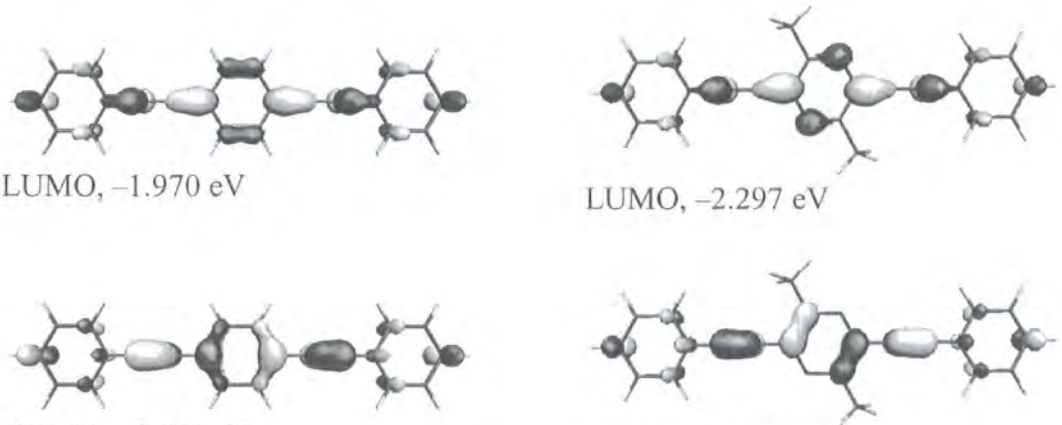

Figure 12 Frontier orbitals of compounds **42** and **37** calculated by B3LYP/6-311G(2d,p) DFT method.

Ph-CC-Ph-CC-Ph	Energy	Ph-CC-Me_2Pz-CC-Ph	Energy
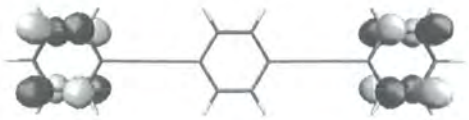	LUMO+4 –0.408 eV	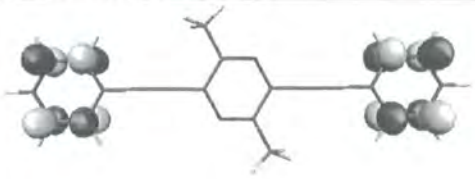	LUMO+4 –0.491 eV
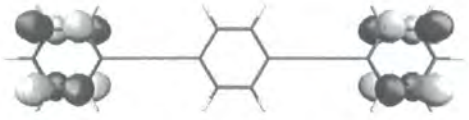	LUMO+3 –0.409 eV	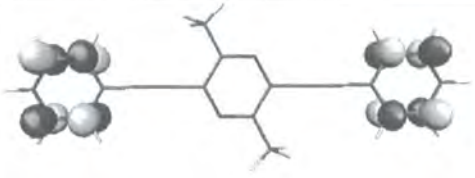	LUMO+3 –0.491 eV
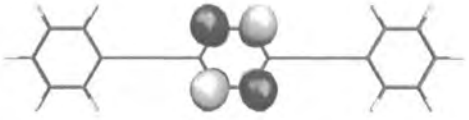	LUMO+2 0.460 eV	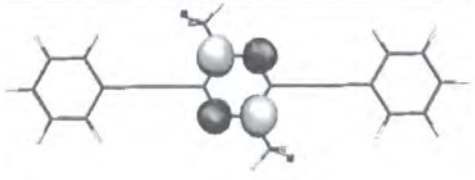	LUMO+2 –0.964 eV
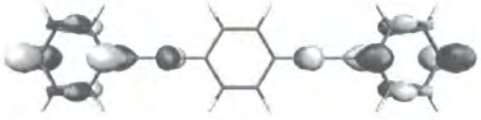	LUMO+1 –0.890 eV	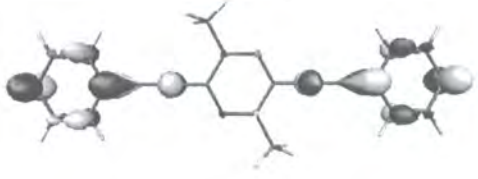	LUMO+1 –1.036 eV
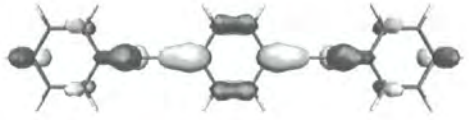	LUMO –1.970 eV	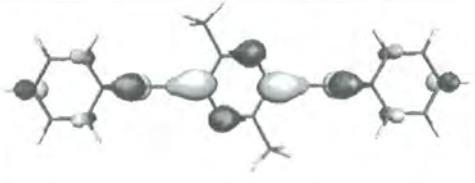	LUMO –2.297 eV
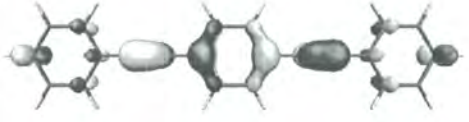	HOMO –5.690 eV	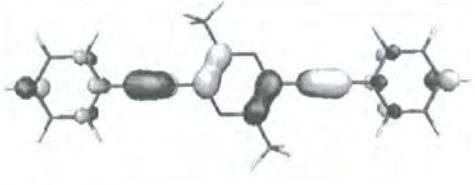	HOMO –5.857 eV
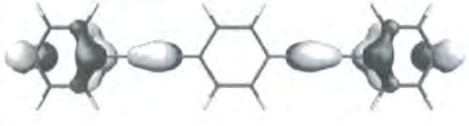	HOMO–1 –6.623 eV	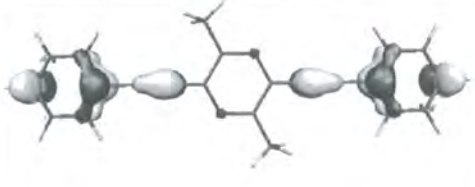	HOMO–1 –6.804 eV

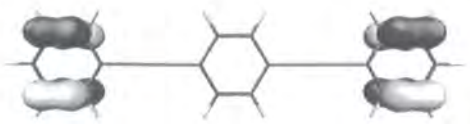	HOMO–2 –7.202 eV		HOMO–2 –6.847 eV
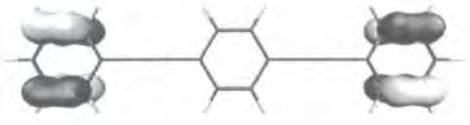	HOMO–3 –7.202 eV	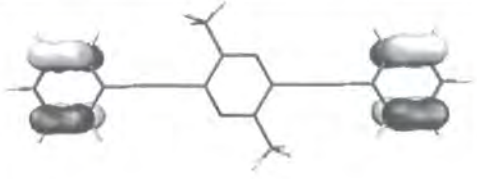	HOMO–3 –7.285 eV
	HOMO–4 –7.307 eV	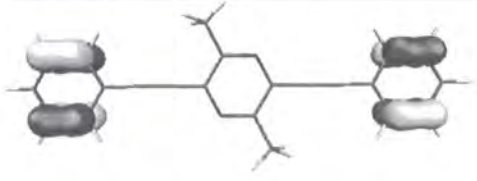	HOMO–4 –7.285 eV

Figure 13 Orbital contour plots for 5 highest occupied MOs and 5 lowest unoccupied MOs in phenylene **42** and in ethylpyrazine derivative **37**.

2.4.4 Cyclic voltammetry

The redox properties of compound **37** were studied by cyclic voltammetry in dry deoxygenated acetonitrile solution. Compound **37** shows irreversible oxidation to the radical cation at +1.62 V vs. Ag/Ag^{+} (Fig. 14). Surprisingly reduction of **37** to its radical anion occurs as a reversible process, although it is observed at quite high negative potentials of ca. –1.87 V. At low scan rate (20–50 mV) the reduction is an irreversible process (not shown on Fig. 14). On increasing of the scan rate to 100 mV s^{-1} it becomes partly reversible (cathodic peak bigger than the anodic peak, $i_c >> i_a$), and at high scan rate of 500 mV s^{-1} the process is almost reversible ($i_c \approx i_a$; ΔE_{pa-pc} = 77 mV, which is close to the theoretical value of 59 mV for a single-electron transfer process). The electrochemical band gap, estimated from the

oxidation and reduction onsets (+1.45 V and –1.78 V) is 3.23 eV, which is in reasonable agreement with the optical band gap estimated from the red edge of the longest wavelength absorption (382 nm = 3.25 eV) and close to the calculated value of the HOMO-LUMO gap (3.56 eV).

The small peaks on the voltammogram observed at near zero potential are probably due to the irreversibility of the oxidation process (and partial reversibility for the reduction) as well as adsorption of the compound on the electrode surface.

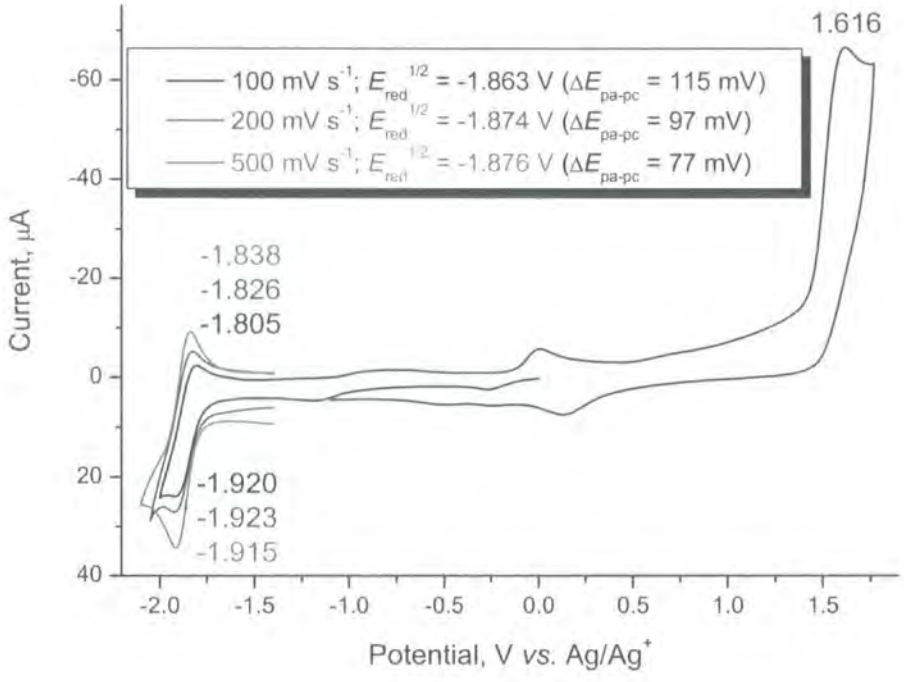

Figure 14 Cyclic voltammogram for dimethylpyrazine derivative **37** in acetonitrile / 0.1 M Bu_4NPF_6 (20 °C) at different scan rates.

2.4.5 Absorption and photoluminescence studies on 37, 38, 40

The absorption and steady state fluorescence spectra in cyclohexane were recorded at ambient temperature for compounds **37**, **38** and **40**.

Normalised of **37** spectra in cyclohexane. Absorbance, excitation for 432 nm emission wavelength, emission for 354 nm excitation wavelength.

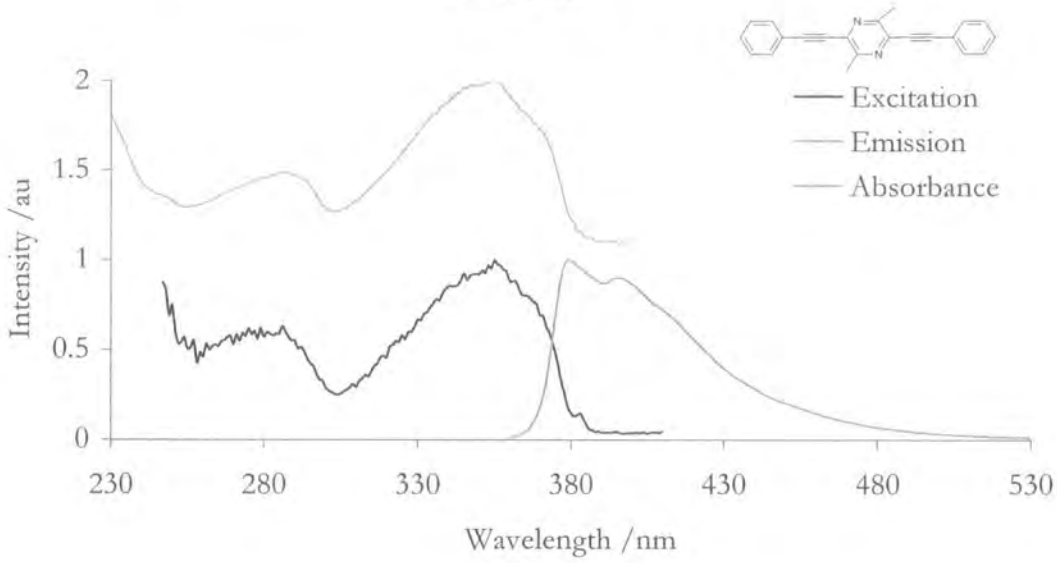

Figure 15

Normalised spectra of **40** in cyclohexane. Absorbance, excitation for 419 nm emission wavelength, emission for 300 nm excitation wavelength.

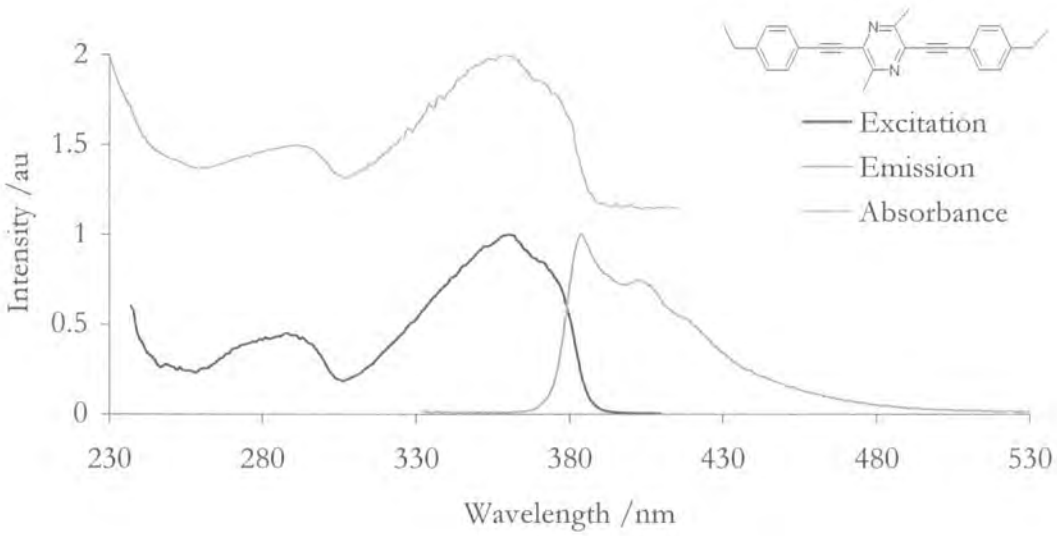

Figure 16

Normalised spectra of **38** in cyclohexane. Absorbance, excitation for 420 nm emission wavelength, emission for 278 nm excitation wavelength.

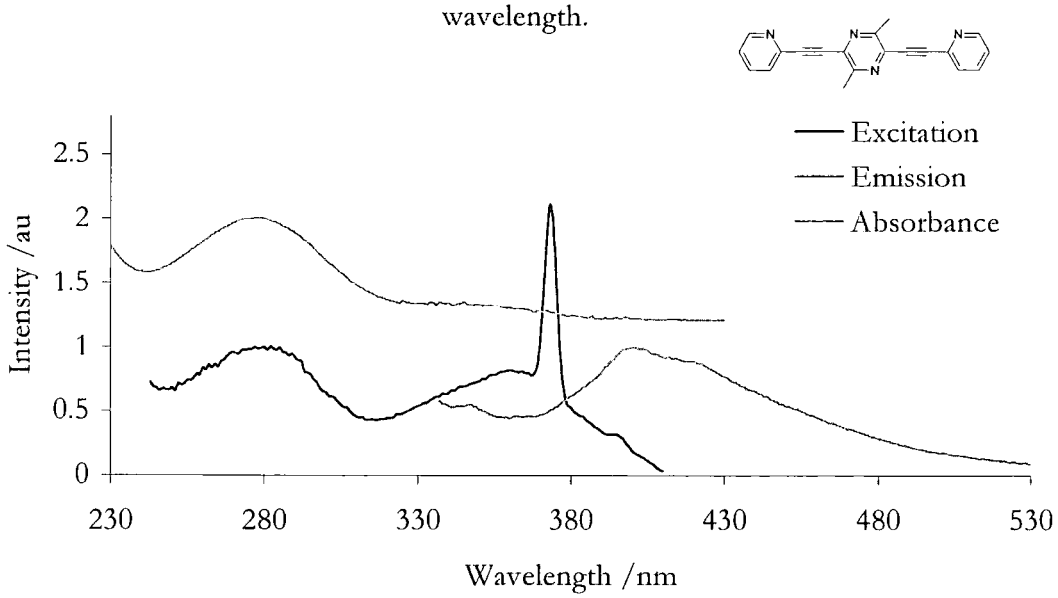

Figure 17

The major absorption, emission and excitation maxima are given in Table 1. The absorbances of these compounds were recorded between 230 nm and 400 nm, and the profiles were devoid of vibrational fine structure. The spectra of **37** and **40** are characterised by two broad bands, with the longer wavelength bands centred at 354 nm and 359 nm for **37** and **40** respectively and are broadly similar to that of observed for 1,4-bis(phenylethynyl)benzene (**42**)[43d]. Compound **38** is characterised by a broad absorbance band at 278 nm.

All emission spectra were found to be independent of excitation wavelength. Compound **37** and **40** show similar fluorescence profiles and the excitation spectra coincide well with the corresponding absorption spectra. There is also a small Stokes shift between the excitation and emission spectra. The emission spectram of **37** and **40** have some vibrational fine

structure and again resemble the spectra observed for **42**. Compound **37** has emission peaks at 379 nm and 395 nm while the emission of **40** is slightly blue shifted with peaks at 384 nm and 403 nm. The difference in the excitation and emission profiles is attributed to differences in the geometric arrangement of the nuclei in the ground and excited states. This is a result of the low barrier to rotation about the alkynly-aryl single bond[43d]. The excitation spectra represent a thermally populated distribution of ground state conformations. The vibrational structure in the emission spectra is indicative of an S_1 state with a larger barrier to rotation from the lowest energy planar orientation of the rings. The ethynyl substituents in **40** only slightly lower the S_1 excited state.

The pyridine substituents have a profound effect on the photophysics of these pyrazine systems. Compound **38** is not very emissive and the excitation and absorption spectra are dissimilar suggesting that the emission arises from an impurity, which could not be detected in the NMR spectra. The excitation spectrum shows two broad bands of similar intensities at 352 nm and 277 nm, which would suggest an extended π-conjugation. However the absorbance at 352 nm is shown to be extremely weak in comparison to the band at 277 nm. The emission spectrum is broad with a peak at 404 nm and is devoid of vibrational structure.

Table 1. The absorption and steady state emission and excitation.

	ABSORPTION	**EMISSION**	**EXCITATION**
37	286(b), 354(b)	379, 395 (b)	283(b), 357(b)
40	291, 359(b), 376(sh)	384, 403, 418	287, 360, 374(sh)
38 Not very emissive	278(b)	404(b)	277(b), 352(b)

Key: b – broad, bw – broad and weak, sh – shoulder

2.5 Conclusions

Efficient synthetic methodology has been developed for the synthesis of diaryleneethynylpyrazine derivatives from commercially available alanine anhydride. Compound **37** has been thoroughly characterised by single crystal X-ray analysis, cyclic voltammetry, absorption and photoluminescence spectra, together with quantum chemical calculations. The presence of the pyrazine unit in the structure enhances the electron accepting properties compared to the phenyl analogue **42.**

These results suggest that future work could involve the use of compound **37** as an electron-transport material in OLED structures. The use of 2,5-dibromo-3,6-dimethylpyrazine **32** as a reagent for new oligoarylene structures should also be explored, cross-coupling methodology.

Chapter Three: Experimental Procedures

This final chapter provides the experimental procedures for the novel compounds presented in this thesis.

3.1 Abbreviations

DCM: methylene dichloride

THF: tetrahydrofuran

$POCl_3$: phosphoryl chloride

CuI: copper(I) iodide

$Pd(PPh_3)_2Cl_2$: dichlorobis(triphennylphosphine)palladium(II)

PBr_3: phosphorus tribromide

$MgSO_4$: magnesium sulfate

NaOH: sodium hydroxide

NMR: Nuclear Magnetic Resonance

MS: Mass Spectrum

3.2 General

3.2.1 Reactions

All reactions which required inert or dry atmospheres, were carried out under a blanket of argon, which was dried by passage through a column of phosphorus pentoxide. THF was

dried according to standard procedures. All reagents employed were of standard reagent grade and purchased from Aldrich and used as supplied.

3.2.2 Analysis

^{1}H NMR spectra were recorded on a Varian VXR 400s at 400 MHz or a Varian Inova 500 at 500 MHz using the deuteriated solvent as lock. Chemical shifts are quoted in ppm, relative to tetramethylsilane (TMS), using TMS or the residual solvent as internal reference. ^{13}C NMR were recorded using broad band decoupling, on the Varian VXR 400s or Varian Inova 500 at 100 MHz and 125 MHz, respectively. The following abbreviations are used in listing NMR spectra: s = singlet, d = doublet, t = triplet, q = quartet.

Electron Impact (EI) mass spectra were recorded on a Micromass AutoSpec spectrometer operating at 70 eV with the ionisation mode as indicated.

An Ati Unicam UV/VIS UV2 spectrometer was used to record the absorption spectra of the samples, which were held in a 1cm path length cuvettes. Emission and excitation spectra were recorded using a Jobin-Yvon Horiba Fluorolog 3-22 Tau-3 spectrofluorimeter. The spectra of dilute solutions with absorbance of less than 0.1 in the 200 nm to 400 nm range were recorded using conventional 90 degree geometry.

The X-ray diffraction experiment was carried out on a Bruker 3-circle diffractometer with a SMART 6K CCD area detector, using graphite-monochromated Mo-K_α radiation ($\overline{\lambda}$ = 0.71073 Å). The crystal was maintained at low temperature (T = 120 K), using a Cryostream (Oxford Cryosystems) open-flow N_2 cryostat. The structure was solved by direct methods

and refined by full-matrix least squares against F^2 of all data, using SHELXTL software. *Crystal data:* $C_{22}H_{16}N_2$, M = 308.37, monoclinic, space group $P2_1/c$ (No. 14), a = 9.059(1), b = 7.515(1), c = 12.102(4) Å, β = 92.33(1)°, U = 823.2(3) Å^3, Z = 2, D_c = 1.244 g cm^{-3}, μ = 0.07 mm^{-1}. Full sphere of reciprocal space was covered by four sets of 0.3° ω scans, each set with different ϕ and/or 2θ angles, yielding 10,887 reflections with $2\theta \leq 55°$, of which 1891 were independent (R_{int} = 0.039). All non-hydrogen atoms were refined in anisotropic approximation, all H atoms were located in a difference Fourier map and refined in isotropic approximation. The refinement of 240 parameters converged at R=0.038 [for 1465 reflections with $F^2 \geq \sigma(F^2)$] and w$R(F^2)$ = 0.115 [for all data].

Cyclic voltammetry experiments were performed on a BAS CV50W electrochemical analyzer with *iR* compensation. Platinum wire, platinum disk (∅ 1.6 mm) and Ag/Ag^+ (0.01 $AgNO_3$ in acetonitrile) were used as counter, working, and reference electrodes, respectively. CV experiments were performed in dry acetonitrile with 0.1 M Bu_4NPF_6 as supporting electrolyte. The scan rate was varied from 50 to 2000 mV s^{-1}. The potentials were referred to Fc/Fc^+ couple as the internal reference, which showed a potential of +0.08 V *vs.* Ag/Ag^+ in our conditions.

3.2.3 Computational procedure

The *ab initio* computations of compounds **42** and **37** were carried out with the Gaussian 98[53] package of programs at both density-functional theory (DFT) levels using Pople's 6–311G split valence basis set supplemented by two *d*-polarisation functions on heavy atoms and *p*-polarisation functions on hydrogens. DFT calculations were carried out using Becke's three-parameter hybrid exchange functional[54] with either Lee–Yang–Parr gradient-corrected correlation functional[55] (B3LYP). Thus, both geometries were optimised with B3LYP/6-

31G(2d,p) and electronic structures were calculated at the same level. Contours of five highest occupied and five lowest unoccupied molecular orbitals were visualised using Molekel v.4.2 program.[56] No constraints of bonds/angles/dihedral angles were applied in the calculations and all the atoms were free to optimise.

3.2.4 Synthetic details

2,5-Dichloro-3,6-dimethylpyrazine 31

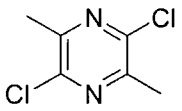

To alanineanlydride **30** (25g 0.176mol) in $POCl_3$ 150ml, PCl_5 9g was added, the mixture was reflux at 105°C for 24h. The mixture was cooled to room temperature, and excess $POCl_3$ was removed by vacuum distillation. Cold brine was added slowly with stirring and a white solid formed after standing for 12 h. Then the mixture was extracted with DCM, and the lower layer was collected. The DCM layer was dried with $MgSO_4$. The solvent in the filtrate was removed by vacuum evaporation and the residue was chromatographed on silica eluted with DCM, followed by crystallization from hexane to yield a white solid of compound **31** (9.3g 31%); m.p. = 73.1-74.1 °C Found C, 40.12; H, 3.78; N, 15. 63%. $C_6H_6Cl_2N_2$ requires C, 40.71 H, 3.42 N, 15.82% MS (EI): m/z 176 (M^+, 100%); δ_H ($CDCl_3$) 2.61 (6 H s CH_3). δ_C ($CDCl_3$) : 21.24 145.60 149.77

2,5-Dibromo-3,6-dimethylpyrazine 32

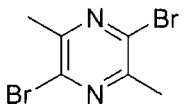

To **31** (5.37g 30mmol), PBr_3 15ml was added. The mixture was stirred at reflux (oil bath temperature 170 °C) for 24h. The mixture was cooled to room temperature, and excess PBr_3 was removed by vacuum distillation. Cold brine was added slowly with stirring and a white solid formed after standing for 12 h. The mixture was extracted with DCM, and the lower layer was collected. The DCM layer was dried by $MgSO_4$. The solvent in the filtrate was removed by vacuum evaporation and the residue was chromatographed on silica eluted with DCM, followed by crystallization from hexane to yield a white solid of compound **32** (2.8g, 35%); m.p. = 84.4-85.8 °C Found C, 26.76; H, 2.52; N, 10.35%. $C_6H_6Br_2N_2$ requires C, 27.10 H, 2.27 N, 10.53% MS (EI): m/z 266 (M^+ 100%); δ_H ($CDCl_3$) 2.58 (6 H s CH_3). δ_C ($CDCl_3$) :22.97 138.80. 152.43

4-[5-(3-Hydroxy-3-methyl-but-1-ynyl)-3,6-dimethylpyrazin-2-yl]-2-methyl-but-3-yn-2-ol 33

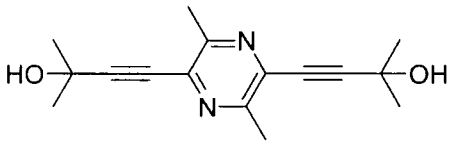

To the solution of 2,5-dibromo-3,6-dimethylpyrazine **32** (0.43g, 1.6mmol) and 2-Methyl-but-3-yn-2-ol (0.4g, 3.2mmol) in dry THF (6.1ml), CuI powder (9.1mg) was added. Triethylamine (0.8ml, 5.7mmol) was added using a syringe, and the solution was stirred at 20°C for 10 min to obtain a clear solution. $Pd(PPh_3)_2Cl_2$ (27mg) was added in one portion and the mixture was stirred at 20°C for 1 h, followed by reflux at 65°C for another 2 h. The

mixture was cooled to room temperature, and the solid formed during the reaction was removed by suction filtration. The solvent in the filtrate was removed by vacuum evaporation and the residue was chromatographed on silica eluted with DCM, followed by crystallization from hexane to yield a yellow solid of compound **33** (0.15g, 35%); m.p. = 170.0-170.8°C Found: C, 70.43; H, 7.67; N, 10.02%. $C_{16}H_{20}N_2O_2$ requires C, 70.56 H, 7.40 N, 10.29%; MS (EI): m/z 272 (M^+, 100%); δ_H ($CDCl_3$) 1.68 (12 H s CH_3) 2.50 (2 H, s OH) 2.60 (6 H s CH_3); δ_C ($CDCl_3$) 21.62 31.04 65.48 79.06 101.29 135.84 152.75

4-(5-Bromo-3,6-dimethylpyrazin-2-yl)-2-methyl-but-3-yn-2-ol 34

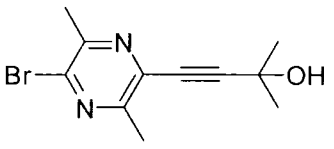

To the solution of 2,5-dibromo-3,6-dimethylpyrazine **32** (0.43g, 1.6mmol) and 2-methyl-but-3-yn-2-ol (0.27g, 1.6mmol) in dry THF (6.1ml), CuI powder (9.1mg) was added. Triethylamine (0.8ml, 5.7mmol) was added using a syringe, and the solution was stirred at 20°C for 10 min to obtain a clear solution. $Pd(PPh_3)_2Cl_2$ (27mg) was added in one portion and the mixture was stirred at 20°C for 1 h, followed by reflux at 65°C for another 1.5 h. The mixture was cooled to room temperature, and the solid formed during the reaction was removed by suction filtration. The solvent in the filtrate was removed by vacuum evaporation and the residue was chromatographed on silica eluted with DCM, followed by crystallization from hexane to yield a yellow solid of compound **34** (0.15g, 36%); m.p. = 168.5-169.1°C Found: C, 48.86; H, 5.13; N, 10.22%. $C_{11}H_{13}BrN_2O$ requires C, 49.09 H, 4.87 N, 10.41%;

MS (EI): m/z 209 (100%), 270 (M^+ 29%); δ_H ($CDCl_3$) 1.63 (6 H s CH_3) 2.60 (1 H, s OH) 2.50 (6 H s CH_3); δ_C ($CDCl_3$) 21.30 23.37 65.53 77.75 100.95 135.95 139.16 151.40 153.71

2,5-Diethynyl-3,6-dimethylpyrazine 35

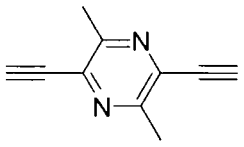

4-[5-(3-Hydroxy-3-methyl-but-1-ynyl)-3,6-dimethylpyrazin-2-yl]-2-methyl-but-3-yn-2-ol **33** (0.51g, 0.2mmol) was added in THF 8ml. NaOH 1.3g was added in the mixture, and the solution was stirred at 20°C for 0.5 h, followed by reflux at 130°C for 2h. The mixture was filtrated, and solid was removed. The solvent in the filtrate was removed by vacuum evaporation and the residue was chromatographed on silica eluted with DCM, solvent was removed by vacuum evaporation and a brown solid was yield of compound **35** (0.07g, 25%); m.p. = 155.1-156.0°C Found: C, 76.67; H, 5.34; N,17.74%. $C_{10}H_8N_2$ requires C, 76.90 H, 5.16 N, 17.94%; MS (EI): m/z 156, (M^+ 100%); δ_H ($CDCl_3$) 2.61 (6 H s CH_3) 3.48 (2 H s CH); δ_C ($CDCl_3$) 21.53 84.38 135.75 153.28

2-Bromo-5-ethynyl-3,6-dimethylpyrazine 36

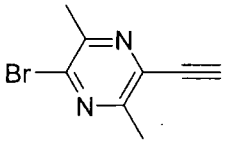

4-(5-Bromo-3,6-dimethylpyrazin-2-yl)-2-methyl-but-3-yn-2-ol **34** (0.32g, 1.2mmol) was added in THF 5ml. NaOH 0.8g was added in the mixture, and the solution was stirred at 20°C for 0.5 h, followed by reflux at 130°C for 2h. The mixture was filtrated, and solid was removed. The solvent in the filtrate was removed by vacuum evaporation and the residue was chromatographed on silica eluted with DCM, solvent was removed by vacuum evaporation and a brown solid was yield of compound **36** (0.06g, 0.23%); m.p. = 144.2-145.1°C Found: C, 45.13; H, 3.55; N, 12.96%. $C_8H_7BrN_2$ requires C, 45.53 H, 3.34 N, 13.27%; MS (EI): m/z 211, (M^+ 100%); δ_H ($CDCl_3$) 2.60 (6H s CH_3) 3.46 (1 H s CH); δ_C ($CDCl_3$) 21. 23.31 83.73 135.24 139.75 151.62 154.09

2,5-Dimethyl-3,6-bis-phenylethynylpyrazine 37

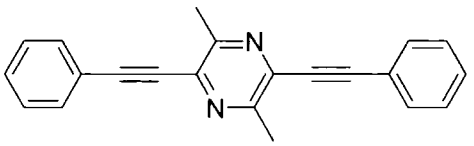

To the solution of 2,5-dibromo-3,6-dimethylpyrazine **32** (0.51g, 2.0 mmol) and ethynyl-benzene (0.49g, 4.8 mmol) in dry THF (7.0 ml), CuI powder (10.6mg) was added. Triethylamine (0.9ml) was added using a syringe, and the solution was stirred at 20°C for 10 min to obtain a clear solution. $Pd(PPh_3)_2Cl_2$ (32mg) was added in one portion and the mixture was stirred at 20°C for 1 h, followed by reflux at 65°C for another 1.5 h. The mixture was cooled to room temperature, and the solid formed during the reaction was removed by suction filtration. The solvent in the filtrate was removed by vacuum evaporation and the residue was chromatographed on silica eluted with DCM, followed by crystallization from hexane to yield a yellow solid of compound **37** (0.25g, 41%); m.p. = 169.1-170.0°C Found: C, 85.44; H, 5.21; N, 9.15%. $C_{22}H_{16}N_2$ requires C, 85.69 H, 5.23 N, 9.08%; MS (EI): m/z 308,

(M^+ 100%); δ_H ($CDCl_3$) 2.69 (6 H s CH_3) 7.32 (6 H s CH) 7.58 (4 H s CH); δ_C ($CDCl_3$) 21.75 86.45 96.72 121.85 128.51 129.49 132.06 136.24 153.02

2,5-Dimethyl-3,6-bis-pyridin-2-ylethynyl-pyrazine 38

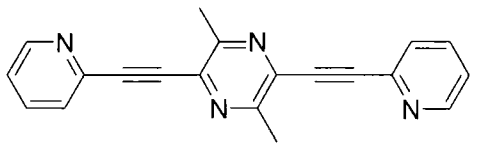

To the solution of 2,5-dibromo-3,6-dimethyl-pyrazine **32** (0.48g, 1.8 mmol) and 1-ethynylpyridine (0.50g, 4.8 mmol) in dry THF (7.0 ml), CuI powder (10.0mg) was added. Triethylamine (0.9ml) was added using a syringe, and the solution was stirred at 20°C for 10 min to obtain a clear solution. $Pd(PPh_3)_2Cl_2$ (30mg) was added in one portion and the mixture was stirred at 20°C for 1 h, followed by reflux at 65°C for another 1.5 h. The mixture was cooled to room temperature, and the solid formed during the reaction was removed by suction filtration. The solvent in the filtrate was removed by vacuum evaporation and the residue was chromatographed on silica eluted with DCM, followed by crystallization from hexane to yield a yellow solid of compound **38** (0.16g, 31%); m.p. = 201.2-201.9°C Found: C,77.24; H, 4.57; N, 17.89%. $C_{20}H_{14}N_4$ requires C, 77.40 H, 4.55 N, 18.05%; MS (EI): m/z 277 (100%), 310 (M^+, 27%); δ_H ($CDCl_3$) 2.60 (6 H s CH_3) 7.31 (2 H s CH) 7.48 (2 H s CH) 8.56 (2 H s CH) ; δ_C ($CDCl_3$) 20.13 72.46 123.31 127.26 135.34 137.42 149.41 153.97

2,5-Bis-biphenyl-4-ylethynyl-3,6-dimethyl-pyrazine 39

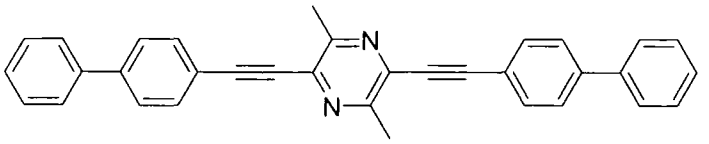

To the solution of 2,5-dibromo-3,6-dimethylpyrazine **32** (0.40g, 1.5 mmol) and 4-ethynyl-biphenyl (0.80g, 4.0 mmol) in dry THF (10.0 ml), CuI powder (8.3mg) was added. Triethylamine (0.8ml) was added using a syringe, and the solution was stirred at 20°C for 10 min to obtain a clear solution. $Pd(PPh_3)_2Cl_2$ (25mg) was added in one portion and the mixture was stirred at 20°C for 1 h, followed by reflux at 65°C for another 1.5 h. The mixture was cooled to room temperature, and the solid formed during the reaction was removed by suction filtration. The solvent in the filtrate was removed by vacuum evaporation and the residue was chromatographed on silica eluted with DCM, followed by crystallization from hexane to yield a yellow solid of compound **39** (0.16g, 24%); m.p. = 188.0-188.7°C ; MS (EI): m/z 460, (M^+ 100%); HRMS (EI) (M+) calcd. for $C_{34}H_{24}N_2$ 460.19395; Found 460.19385; δ_H ($CDCl_3$) 2.62 (6 H s CH_3) 7.18 (2 H s CH) 7.29 (4 H s CH) 7.38 (8 H s CH) 7.61 (4 H s CH); δ_C ($CDCl_3$) 14.68 74.66 81.84 120.63 127.07 127.14 127.88 128.93 132.97 140.10 141.97 156.91

2,5-Bis-(4-ethyl-phenylethynyl)-3,6-dimethyl-pyrazine 40

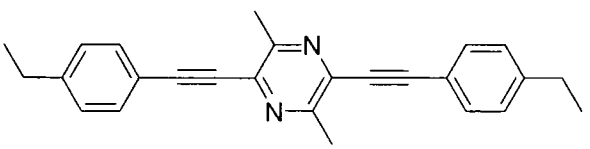

To the solution of 2,5-dibromo-3,6-dimethylpyrazine **32** (0.44g, 1.6 mmol) and 1-ethyl-4-ethynyl-benzene (0.65g, 5.0 mmol) in dry THF (7.0 ml), CuI powder (9.1mg) was added.

Triethylamine (0.8ml) was added using a syringe, and the solution was stirred at 20°C for 10 min to obtain a clear solution. $Pd(PPh_3)_2Cl_2$ (27mg) was added in one portion and the mixture was stirred at 20°C for 1 h, followed by reflux at 65°C for another 1.5 h. The mixture was cooled to room temperature, and the solid formed during the reaction was removed by suction filtration. The solvent in the filtrate was removed by vacuum evaporation and the residue was chromatographed on silica eluted with DCM, followed by crystallization from hexane to a yield yellow solid of compound **40** (0.22g, 38%); m.p. = 196.5-198.3°C MS (EI): m/z 364, (M^+ 100%); HRMS (EI) (M+) calcd. for $C_{26}H_{24}N_2$ 364.19395; Found 364.19400; δ_H ($CDCl_3$) 1.19 (6 H t J = 7.6 Hz CH_3) 2.62 (4 H q J = 7.6 Hz CH_2) 2.68 (6 H s CH_3) 7.15 (4H d J = 8 Hz CH) 7.48 (4H d J = 8 Hz CH); δ_C ($CDCl_3$)15.89 22.15 29.78 86.20 97.81 119.73 128.22 132.31 136.23 148.34 152.68

2,5-Bis-(4-chloro-phenylethynyl)-3,6-dimethyl-pyrazine 41

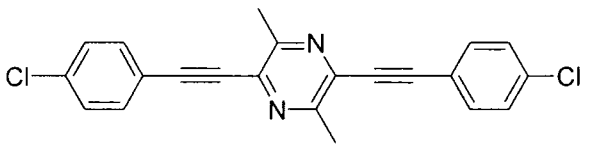

To the solution of 2,5-dibromo-3,6-dimethylpyrazine **32** (0.45g, 1.7 mmol) and 1-chloro-4-ethynyl-benzene (0.52g, 3.8 mmol) in dry THF (7.0 ml), CuI powder (9.3mg) was added. Triethylamine (0.8ml) was added using a syringe, and the solution was stirred at 20°C for 10 min to obtain a clear solution. $Pd(PPh_3)_2Cl_2$ (28mg) was added in one portion and the mixture was stirred at 20°C for 1 h, followed by reflux at 65°C for another 1.5 h. The mixture was cooled to room temperature, and the solid formed during the reaction was removed by suction filtration. The solvent in the filtrate was removed by vacuum evaporation and the residue was chromatographed on silica eluted with DCM, followed by crystallization from

hexane to a yield yellow solid of compound **41** (0.14g, 23%); m.p. = 190.5-191.1°C MS (EI): m/z 270 (100%), 376(M^+, 58%); HRMS (EI) (M+) calcd. for $C_{22}H_{14}Cl_2N_2$ 376.05340; Found 376.05329; δ_H ($CDCl_3$) 2.69 (6 H s CH_3) 7.31 (4 H s CH) 7.48 (4 H s CH) δ_C ($CDCl_3$) 20.93 74.66 81.84 120.63 127.20 133.21 141.56 156.45

References

[1] Handbook of Conducting Polymers T. A. Skotheim R. L. Elsenbaumer and J. R. Reynolds (Editors) 2nd Edition, Marcel Dekker, New York, 1998

[2] (a) H. Koezuka, A. Tsumara and T. Ando, *Synth. Met.* **1987**, *18*, 699; (b) A. Assadi, C. Svensson, M. Willander and O. Inganäs, *Appl. Phys. Lett.* **1988**, *53*, 195

[3] Electronic Materials: The Oligomer Approach, K. Müllen and G. Wegner (Editors) Wiley-VCH, Weinheim, 1998

[4] Y. A. Ono, Electroluminescence in Encyclopedia of Applied Physics, G. L. Trigg (Editors), VCH, Weinheim, 1993, vol. 5, p. 295

[5] G. Destriau, *J. Chim. Phys.*, 1936, **33**, 587

[6] M. Pope, H. P. Kallmann and P. Magnante, *J. Chem. Phys.*, 1963, **38**, 2042

[7] C. W. Tang and S. A. VanSlyke, *Appl. Phys. Lett.*, 1987, **51**, 913

[8] J. H. Burroughes, D. D. C. Bradley, A. R. Brown, R. N. Marks, K. Mackay, R. H. Friend, P. L. Burn and A. B. Holmes, *Nature*, 1990, **347**, 539

[9] G.Leising, S. Tasch and W. Graupner, Fundamentals of Electroluminescence in Paraphenylene-type Conjugated Polymers and Oligomers in reference 1, p. 847.

[10] D. Z. Garbuzov, V. Bulovic, P. E. Burrows and S. R. Forrest, *Chem. Phys. Lett.*, 1996, **249**, 433

[11] (a) C. H. Chen, J. Shi and C. W. Tang, *Macromol. Symp.*, 1997, **125**, 1.; (b) C. H. Chen and J. Shi, *Coord. Chem. Rev.*, 1998, **171**, 161; (c) J. Kido and J. Endo, *Chem. Lett.*, 1997, 593

[12] (a) Y. Hamada, T. Sano, M. Fujita, T. Fujii, Y. Nishio and K. Shibata, *Jpn. J. Appl. Phys.*, 1993, **32**, L514 (b) Y. Hamada, T. Sano, M. Fujita, T. Fujii, Y. Nishio and K. Shibata, *Chem. Lett.*, 1993, 905 (c) Y. Hamada, H. Kanno, T. Sano, H. Fujii, Y. Nishio, H. Takahashi, T. Usuki and K. Shibata, *Appl. Phys. Lett.*, 1998, **72**, 1939

[13] (a)D.-G. Ma, D.-K. Wang, Z.-Y. Hong, X.-J. Zhao, X.-B. Jing, F.-S. Wang, B. Li, H.-J. Zhang and S.-B. Wang, *Chin. J. Chem.*, 1998, **16**, 1 (b) C. Liang, W. Li, Z. Hong, X. Liu, J. Peng, L. Liu, Z. Liu, J. Yu, D. Zhao and S.-T. Lee, *Synth. Met.*, 1997, **91**, 275 (c) S. Dirr, S. Wiese, H.-H. Johannes, D. Ammermann, A. Böhler, W. Grahn and W. Kowalsky, *Synth. Met.*, 1997, **91**, 53

[14] X. T. Tao, H. Suzuki, T. Wada, S. Miyata and H. Sasabe, *J. Am. Chem. Soc.*, 1999, **121**, 9447

[15] Y. Hamada, T. Sano, M. Fujita, T. Fujii, Y. Nishio and K. Shibata, *Jpn. J. Appl. Phys.*, 1993, **32**, L514

[16] Y. Hamada, T. Sano, M. Fujita, T. Fujii, Y. Nishio and K. Shibata, *Chem. Lett.*, 1993, 905

[17] C. Liang, W. Li, Z. Hong, X. Liu, J. Peng, L. Liu, Z. Liu, J. Yu, D. Zhao and S.-T. Lee, *Synth. Met.*, 1997, **91**, 275

[18] S. Dirr, S. Wiese, H.-H. Johannes, D. Ammermann, A. Böhler, W. Grahn and W. Kowalsky, *Synth. Met.*, 1997, **91**, 53

[19] C. W. Tang, S. A. VanSlyke and C. H. Chen, *J. Appl. Phys.*, 1989, **65**, 3610

[20] (a) Z.-I. Zhang, X.-Y. Jiang, S.-H. Xu, T. Nagatomo and O. Omoto, *J. Phys. D: Appl. Phys.*, 1998, **31**, 32; (b) Z.-I. Zhang, X.-Y. Jiang, S.-H. Xu, T. Nagatomo and O. Omoto, *Synth. Met.*, 1997, **91**, 131

[21] (a) M. Thelakkat and H.-W. Schmidt, *Polym. Adv. Technol.*, 1998, **9**, 429 (b) T. Tsutsui, E.-I. Aminaka, Y. Fujita, Y. Hamada and S. Saito, *Synth. Met.*, 1993, **55-57**, 4157

[22] Y. Cao, I. D. Parker, G. Yu, C. Zhang and A. J. Heeger, *Nature*, 1999, **397**, 414

[23] J. Kido, C. Ontaki, K. Hongawa, K. Oknyama and K. Nagai, *Jpn. J. Appl. Phys.*, 1993, **32**, L917

[24] S. Pfeiffer, H.-H. Hörhold, H. Boerner, H. Nikol and W. Busselt, *Proc. SPIE Int. Soc. Opt. Eng.*, 1998, **258**, 3476

[25] A. Kraft, A. C. Grimsdale and A. B. Holmes, *Angew. Chem., Int. Ed.*, 1998, **37**, 402

[26] N. Tamoto, C. Adachi and K. Nagai, *Chem. Mater.*, 1997, **9**, 1077

[27] D. Braun and A. J. Heeger, *Appl. Phys. Lett.*, 1991, **58**, 1982

[28] J. Salbeck, *Ber. Bunsenges. Phys. Chem.*, 1996, **100**, 1666

[29] G. Grem, G. Leditzky, B. Ullrich and G. Leising, *Synth. Met.*, 1992, **51**, 383

[30] (a) A. Edwards, S. Blumstengel, I. Sokolik, H. Yun, Y. Okamoto and R. Dorsinville, *Synth. Met.*, 1997, **84**, 639; (b) J. Birgerson, M. Fahlman, P. Bröms and W. R. Salaneck, *Synth. Met.*, 1996, **80**, 125

[31] G. Grem, C. Paar, J. Stampfl, G. Leising, J. Huber and U. Scherf, *Chem. Mater.*, 1995, **7**, 2

[32] E. J. W. List, L. Holzer, S. Tasch, G. Leising, U. Scherf, K. Müllen, M. Catellani and S. Luzzati, *Solid State Commun.*, 1999, **109**, 455

[33] (a) E. Ettedgui, G. T. Davis, B. Hu and F. E. Karasz, *Synth. Met.*, 1997, **90**, 73; (b)M. Kawaharada, M. Ooishi, T. Saito and E. Hasegawa, *Synth. Met.*, 1997, **91**, 113; (c) J. R. Rasmusson, P. Bröms, J. Birgerson, R. Erlandsson and W. R. Salaneck, *Synth. Met.*, 1996, **79**, 75

[34] (a) J. C. Scott, J. H. Kaufman, P. J. Brock, R. DiPietro, J. Salem and J. A. Goitia, *J. Appl. Phys.*, 1996, **79**, 2745; (b) J. Manca, W. Bijnens, R. Kiebooms, J. D'Haen, M. D'Olieslaeger,

T.-D. Wu, W. De Ceuninck, L. De Schepper, D. Vanderzande, J. Gelan and L. Stals, *Opt. Mater.*, 1998, **9**, 134; (c) B. H. Cumpston, I. D. Parker and K. F. Jensen, *J. Appl. Phys.*, 1997, **81**, 3716; (d) L. J. Rothberg, M. Yan, S. Son, M. E. Galvin, E. W. Kwock, T. M. Miller, H. E. Katz, R. C. Haddon and F. Papadimitrakopoulos, *Synth. Met.*, 1996, **78**, 231; (e) V. N. Savvate'ev, A. V. Yakimov, D. Davidov, R. M. Pogreb, R. Neumann and Y. Avny, *Appl. Phys. Lett.*, 1997, **71**, 3344

[35] (a) D. Zou, M. Yahiro and T. Tsutsui, *Appl. Phys. Lett.*, 1998, **72**, 2484; (b) H. Antoniadis, M. R. Hueschen, J. N. Miller, R. L. Moon, D. B. Roitman and J. R. Sheats, *Macromol. Symp.*, 1997, **125**, 59; (c) D. Zou, M. Yahiro and T. Tsutsui, *Synth. Met.*, 1997, **91**, 191

[36] (a) D. O'Brien, M. S. Weaver, D. G. Lidzey and D. D. C. Bradley, *Appl. Phys. Lett.*, 1996, **69**, 881; (b) Z. B. Deng, S. T. Lee, L.-C. Chen, S.-Z. Dong, H.-H. Sun and X. Wang, *Acta Phys. Sin. Overseas Ed.*, 1997, **6**, 921; (c) M. S. Weaver, D. G. Lidzey, T. A. Fisher, M. A. Pate, D. O'Brien, A. Bleyer, A. Tajbakhsh, D. D. C. Bradley, M. S. Skolnick and G. Hill, *Thin Solid Films*, 1996, **273**, 39

[37] (a) D. D. Gebler, Y. Z. Wang, J. W. Blatchford, S. W. Jessen, L. B. Lin, T. L. Gustafson, H. L. Wang, T. M. Swager, A. G. MacDiarmid and A. J. Epstein, *J. Appl. Phys.*, 1995, **78**, 4264; (b) Yu Liu, Jianhua Guo, Jing Feng, Huidong Zhang, Yanqin Li and Yue Wang, *Appl. Phys.Lett.*, 2001, **78**, 2300

[38] C. Wang, M. Kilitziraki, J. A. H. MacBride, M. R. Bryce, L. Horsburgh, A. Sheridan, A. P. Monkman and I. D. W. Samuel, *Adv. Mater.*, 2000, **12**, 217

[39] S-S. Ng, H-F, Lu, H.S.O. Chan, A. Fujii, T. Laga and K. Yoshino, *Adv. Mater.*, 2000, **12**, 1122

[40] K-T. Wong, T. S. Hung, Y. Lin, C-C. Wu, G-H. Lee, S-M. Peng, C. H. Chou and Y. O. Su, *Org. Lett.* 2002, **4**, 513

[41] F. Turksoy, G. Hughes, A. S. Batsanov and M. R. Bryce *J. Mater. Chem.*, 2003, **13**, 1554

[42] Z. Peng; M. E. Galvin, *Chem. Mater.* 1998, **10**, 1785

[43] (a) U. H. F. Bunz, *Chem. Rev.*, 2000, **100**, 1605; (b) S. Anderson, *Chem. Eur. J.*, 2001, **7**, 4706; (c) A. P. H. J. Schenning, A. C. Tsipsis, S. C. J. Meskers, D. Beljonne, E. W. Meijer and J. L. Brédas, *Chem. Mater.*, 2002, **14**, 1362; (d) A. Beeby, K. Findlay, P. J. Low and T. B. Marder, *J. Am. Chem. Soc.*, 2002, **124**, 8280

[44] Z. J. Donhauser, B. A. Mantooth, K. F. Kelly, L. A. Bumm, J. D. Monnell, J. J. Stapleton, D. W. Price, A. M. Rawlett, D. L. Allara, J. M. Tour and P. S. Weiss, *Science*, 2001, **292**, 2303.

[45] (a) R. C. Ellingson and R. L. Henry, *J. Am. Chem. Soc.*, 1949, **71**, 2798; (b) K. Pieterse, J. A. J. M. Vekemans, H. Kooijman, A. J. Spek and E. J. Meijer, *Chem. Eur. J.*, 2000, **6**, 4597

[46] G. Hughes, personal communication

[47] F. Ogura, Y. Hama, Y. Aso and T. Otsubo, *Synth. Met.*, 1988, **27**, B295

[48] K. W. Blake and P. G. Sammes, *J. Chem. Soc. (C),* 1970, 1070

[49] F. Ogura, Y. Hama, Y. Aso and T. Otsabo, *Synth. Met.* 1988, **27**, B295

[50] (a) K. Sonogashira, Y. Tohda and N. Hagihara, *Tetrahedron Lett.*, 1975, **50**, 4467; (b) K. Sonogashira, in *Comprehensive Organic Synthesis*, Vol. 3, Pergamon Press, 1990, p. 521

[51] I. J. S. Fairlamb, P. S. Bäuerlein, L. R. Marrison and J. M. Dickinson, *Chem. Commun.*, 2003, 632

[52] Single crystal X-ray diffraction data for compound **42** are from: T. B. Marder, private communication.

[53] M. J. Frisch, G. W. Trucks, H. B. Schlegel, G. E. Scuseria, M. A. Robb, J. R. Cheeseman, V. G. Zakrzewski, J. A. Montgomery, Jr., R. E. Stratmann, J. C. Burant, S. Dapprich, J. M. Millam, A. D. Daniels, K. N. Kudin, M. C. Strain, O. Farkas, J. Tomasi, V. Barone, M. Cossi, R. Cammi, B. Mennucci, C. Pomelli, C. Adamo, S. Clifford, J. Ochterski, G. A. Petersson, P. Y. Ayala, Q. Cui, K. Morokuma, D. K. Malick, A. D. Rabuck, K. Raghavachari, J. B. Foresman, J. Cioslowski, J. V. Ortiz, A. G. Baboul, B. B. Stefanov, G. Liu, A. Liashenko, P. Piskorz, I. Komaromi, R. Gomperts, R. L. Martin, D. J. Fox, T. Keith, M. A. Al-Laham, C. Y. Peng, A. Nanayakkara, M. Challacombe, P. M. W. Gill, B. Johnson, W. Chen, M. W. Wong, J. L. Andres, C. Gonzalez, M. Head-Gordon, E. S. Replogle and J. A. Pople, Gaussian 98, Revision A.9, Gaussian, Inc., Pittsburgh PA, 1998.

[54] A. D. Becke, *Phys. Rev. A*, 1988, **38**, 3098; A. D. Becke, *J. Chem. Phys.*, 1993, **98**, 5648.

[55] C. Lee, W. Yang and R. G. Parr, *Phys. Rev. B*, 1988, **37**, 785.

[56] (a) P. Flükiger, H. P. Lüthi, S. Portmann and J. Weber, Molekel, Version 4.2, Swiss Center for Scientific Computing, Manno (Switzerland), 2000, http://www.cscs.ch/molekel/; (b) S. Portmann and H. P. Lüthi, *Chimia*, 2000, **54**, 766.